Government of **Western Australia**
Department of **Mines and Petroleum**

RECORD 2015/12

THE WINDIMURRA IGNEOUS COMPLEX, YILGARN CRATON: AN ARCHEAN LAYERED INTRUSION REVEALED BY SEISMIC DATA AND 3D MODELLING

by
TJ Ivanic and J Brett



Geological Survey
of Western Australia

Government of Western Australia
Department of Mines and Petroleum

Record 2015/12

THE WINDIMURRA IGNEOUS COMPLEX, YILGARN CRATON: AN ARCHEAN LAYERED INTRUSION REVEALED BY SEISMIC DATA AND 3D MODELLING

by
TJ Ivanic and J Brett

Perth 2015

Geological Survey of
Western Australia

MINISTER FOR MINES AND PETROLEUM
Hon. Bill Marmion MLA

DIRECTOR GENERAL, DEPARTMENT OF MINES AND PETROLEUM
Richard Sellers

EXECUTIVE DIRECTOR, GEOLOGICAL SURVEY OF WESTERN AUSTRALIA
Rick Rogerson

REFERENCE
The recommended reference for this publication is:

Ivanic, TJ and Brett, J 2015, The Windimurra Igneous Complex, Yilgarn Craton: an Archean layered intrusion revealed by seismic data and 3D modelling: Geological Survey of Western Australia, Record 2015/12, 28p.

National Library of Australia Card Number and ISBN 978-1-74168-640-1

Grid references in this publication refer to the Geocentric Datum of Australia 1994 (GDA94). Locations mentioned in the text are referenced using Map Grid Australia (MGA) coordinates, Zone 50. All locations are quoted to at least the nearest 100 m.

Published 2015 by Geological Survey of Western Australia
This Record is published in digital format (PDF) and is available online at <www.dmp.wa.gov.au/GSWApublications>.

Further details of geological products and maps produced by the Geological Survey of Western Australia are available from:
Information Centre
Department of Mines and Petroleum
100 Plain Street
EAST PERTH WESTERN AUSTRALIA 6004
Telephone: +61 8 9222 3459 Facsimile: +61 8 9222 3444
www.dmp.wa.gov.au/GSWApublications

Contents

Figures

Tables

Appendix*

---

*The 3D geomodel to accompany this Record is provided separately on a USB. The Record may be accessed directly on our website independent of the USB.

The Windimurra Igneous Complex, Yilgarn Craton: an Archean layered intrusion revealed by seismic data and 3D modelling

by

TJ Ivanic and J Brett

Abstract

The Windimurra Igneous Complex is situated in the western part of the Archean Yilgarn Craton, Western Australia within the Youanmi Terrane. It is part of the plume-related and laterally extensive c. 2.81 Ga Meeline Suite, an anhydrous tholeiitic suite comprising five layered mafic–ultramafic intrusions 25–80 km in diameter. The intrusions also host significant V–Ti mineralization in their fractionated, Fe-rich upper zones. The Windimurra Igneous Complex is the only intrusion to contain two upper zones, separated by the Shephards Discordant Zone. Recent mapping, aeromagnetic and gravity surveys, and the Youanmi Seismic lines have provided unparalleled 3D constraints on the Windimurra Igneous Complex. These data have allowed direct assessment of the zone thicknesses and facilitated construction of a 3D model. This model was refined by forward modelling of potential field data and tested against a geophysical inversion. The results show that the complex is thicker than previously predicted at approximately 11 km, which make it the thickest layered mafic–ultramafic intrusion identified globally. Relative to the consistency of layered igneous units, three significantly discordant units are identified: (1) the Shephards Discordant Zone separating the older, basal eastern lobe from the western lobe; (2) the base of the highly transgressive upper zone of the western lobe; (3) the roof zone and overlying Kantie Murdana Volcanics Member. The geometry of these three features provides constraints on a multistage genetic model for magma emplacement. In addition, the indication of a thick, subsurface ultramafic zone provides a potential target for Ni–Cr–PGE mineralization.

KEYWORDS: layered intrusions, Archaean, magma chamber, magmatic deposits,Youanmi Terrane

Introduction

Layered mafic–ultramafic intrusions are host to a variety of ore deposits such as Ti–V and Ni–Cr–Cu–PGE (Platinum Group Elements). These deposits are associated with magma chamber processes and influenced, in particular, by cumulate layering geometry. Therefore, it is essential to understand the large-scale primary 3D geometry of these intrusions in order to assess the nature of magma chamber processes and prospectivity for ore deposit formation.

The Windimurra Igneous Complex (WIC) is a giant layered mafic–ultramafic intrusion ~2500 km^2 (85 km north–south by 37 km east–west) located in the central Youanmi Terrane, Yilgarn Craton, Western Australia (Fig. 1). It is the largest, relatively intact and exposed, mafic–ultramafic intrusion in Australia. Recent work has directly dated the complex and assigned it to the c. 2813 Ma, anhydrous Meeline Suite (Ivanic et al., 2010; Wingate et al., 2012), which includes other large layered mafic–ultramafic intrusions such as the Youanmi Igneous Complex (YIC). The Meeline Suite intrudes into the Norie Group of the Murchison Supergroup (Van Kranendonk et al., 2013). It is widely regarded that these intrusions are the results of a mantle plume affecting a wide region of the Yilgarn Craton (Ivanic et al., 2010; Wyche et al., 2012; Wyman and Kerrich, 2012; Van Kranendonk et al., 2013). The central–northern part of the WIC (Fig. 2) is overlain by the rhyolitic Kantie Murdana Volcanics Member of the Yaloginda Formation of the Norie Group. These rhyolitic volcanics have also been directly dated at 2813 ± 3 Ma (Nelson, 2001). There are several economic vanadium deposits hosted within the magnetitites of the upper zone (Fig. 3).

The WIC is dissected by larger shear zones (e.g. Challa Shear Zone and Yarloo Shear Zone) and also smaller brittle faults. Hence parts of the WIC occur as sheared lenses to the south and east of the main body, especially east of the Challa Shear Zone (unassigned gabbros, Fig. 2). Based on aeromagnetic images, these features are mapped as up to 25 km north–south and 5 km east–west lenses (Figs 2 and 4).

There is an overall progression from more mafic rocks in the lower zone to large volumes of leucocratic rocks in the middle and upper zones (Figs 5 and 6). Within these zones, megacyclicity on an approximately 200 m scale

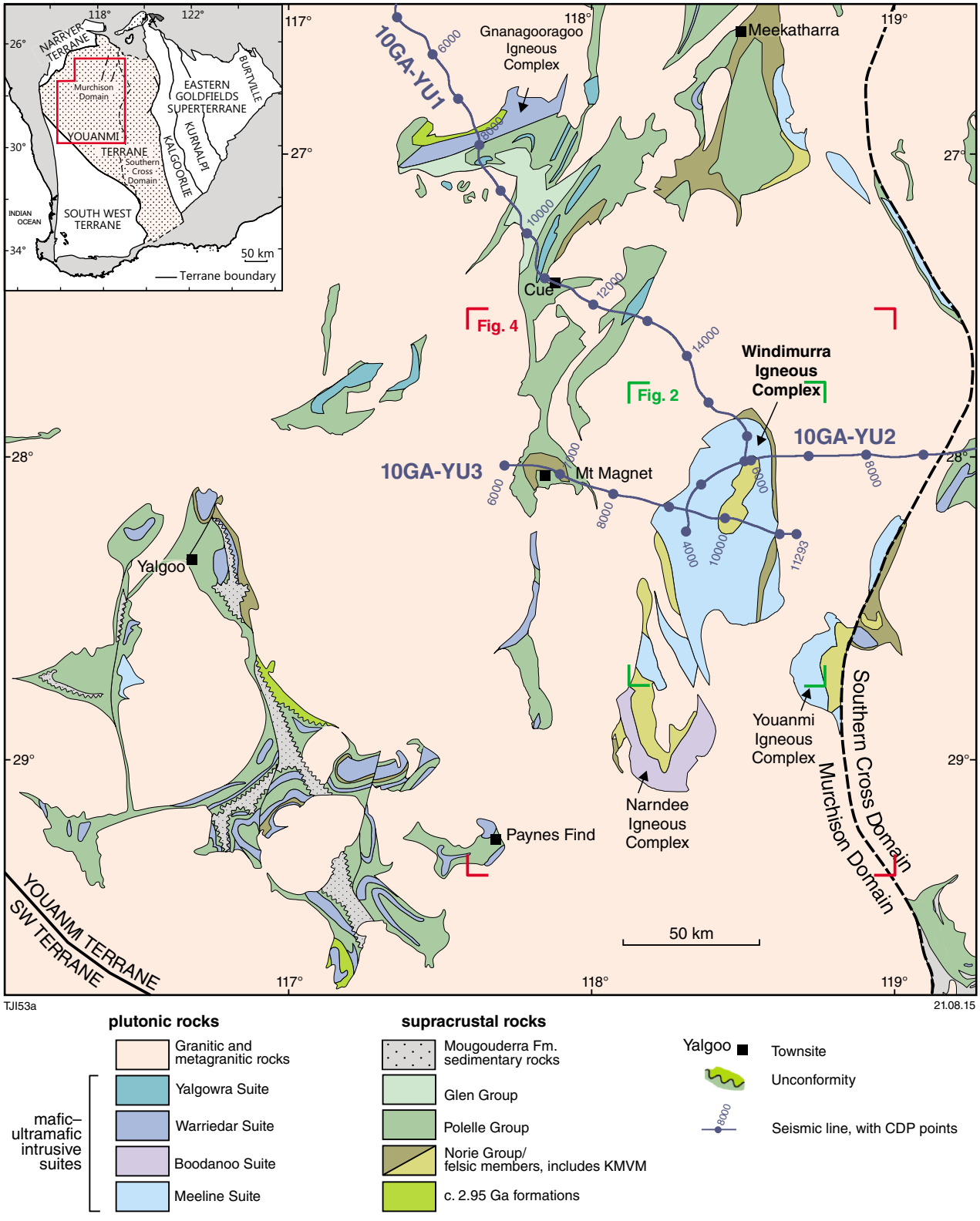

Figure 1. **Simplified geological map of the northern Murchison Domain, highlighting the location of mafic–ultramafic intrusive suites relative to supracrustal greenstone groups and granitic rocks. Also shown are the locations of the three seismic lines (10GA-YU1, 10GA-YU2, 10GA-YU3). Modified from (Ivanic et al., 2010). Inset shows broader setting of the Murchison Domain within the Youanmi Terrane of the Yilgarn Craton. KMVM = Kantie Murdana Volcanics Member of the Yaloginda Formation. Corner extents of Figures 2 and 4 indicated in green and red, respectively.**

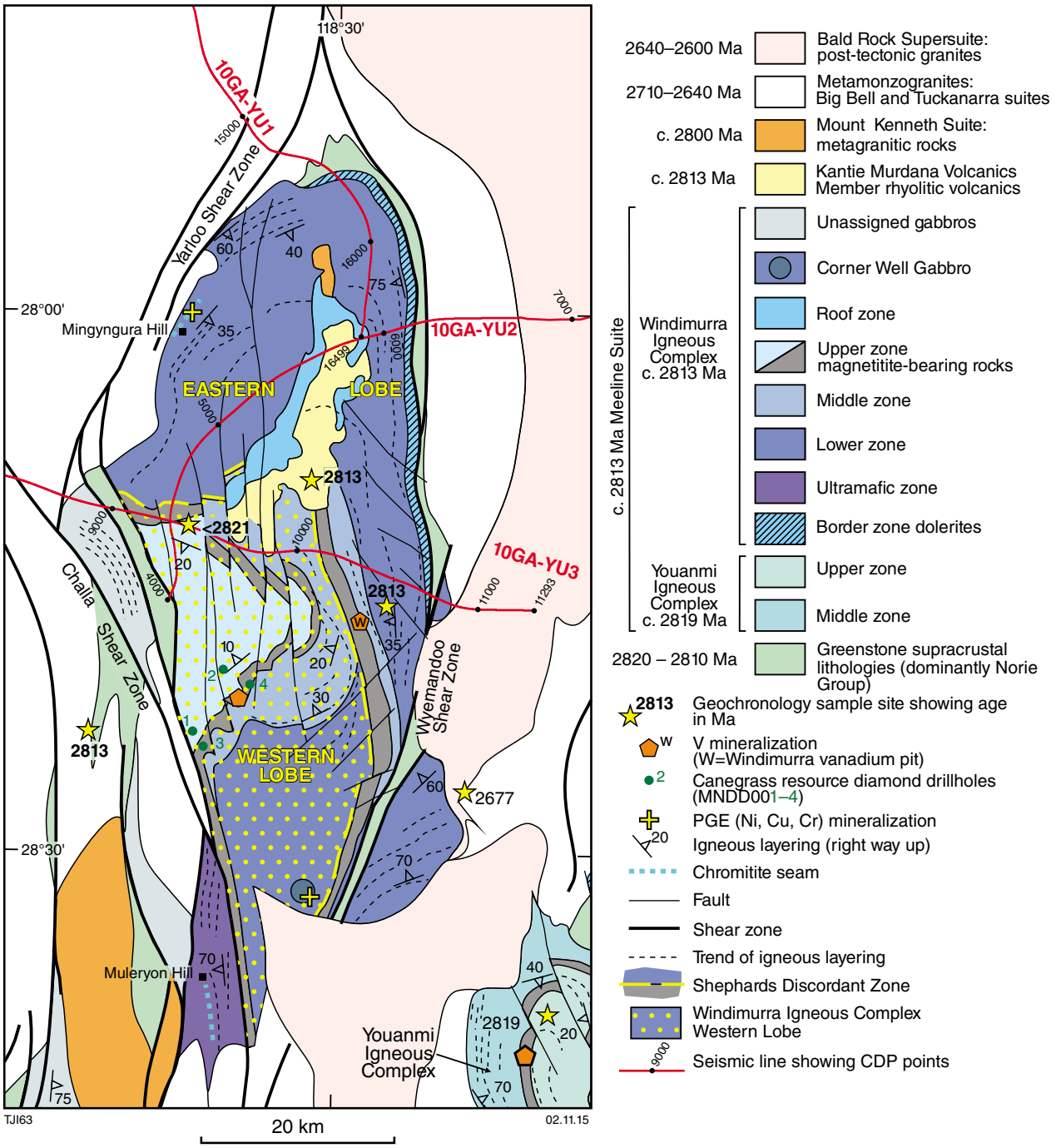

Figure 2. Interpreted geological map of the Windimurra Igneous Complex, highlighting available geochronological data and mineralization styles. Note the location of the Shephards Discordant Zone separating the eastern and western lobes and the location of three seismic lines (10GA-YU1, 10GA-YU2, 10GA-YU3). Area of map is a few kilometres wider than that of the modelled volume (Fig. 9), which does not include modelling of the Youanmi Igneous Complex, shown here to the southeast. The 3D geomodel layer 'Images–Geological maps' represents the original input data for the 3D geomodel and is superceded here.

TJI64 10.06.15

Figure 3. Photograph looking south in the Windimurra vanadium pit showing moderately west-dipping layers of magnetitite (dark layers) hosted in magnetite-bearing leucogabbro (pale layers) of the upper zone of the eastern lobe. Pit wall is 30 m high. Note the multiscale cyclicity of mafic and felsic layers creating a heterogeneous rock volume on a centimetre-to-decametre scale.

can be related to at least 13 documented reversals in the chemostratigraphy (Ahmat, 1986). The exposed complex has an extremely felsic overall composition compared to other layered gabbros worldwide and has been described as a having an anorthositic affinity (Ahmat and De Laeter, 1982) and a high Ca–Fe tholeiitic composition (Ahmat, 1986). However, it is possible that its composition is more typically tholeiitic (c.f. Nebel et al., 2013a) if it can be shown that a large volume of ultramafic zone material exists at depth.

Previous work

Previous work documenting the geometry of the complex involved 1:50 000 surface mapping of igneous and structural data (Ahmat, 1986), which concluded that the form of the WIC was tabular and broadly comprised inwardly dipping igneous layering. This work included forward modelling two gravity transects set in a regional, low-resolution, gravity survey area covering the WIC. The gravity modelling utilized simple slabs of estimated densities and concluded that the WIC extended down to an average of 3 km depth and locally down to 5 km in the vicinity of these transects. This was clearly at odds with the cumulative stratigraphic thickness logged at 13 km from surface observations (Fig. 5). This discrepancy was explained by the presence of significant discordant features, which were mapped throughout the lower, middle and upper zones including the Shephards Discordant Zone (SDZ) (see further discussions below). The Kantie Murdana Volcanics Member (including 'mafic intrusives' presumably of what we now call the roof zone of the WIC), was modelled to extend down to a maximum of 1.5 km depth.

New gravity and magnetic survey data acquired from 2004 onwards greatly improved the resolution of coverage over the WIC area. The magnetic surveys have a line spacing of 400 m, gridded at a resolution of 80 m. The gravity surveys have a data spacing of 2.5 km, gridded at a resolution of 400 m.

Recent and extensive mapping at 1:100 000 scale (simplified in Fig. 2) incorporated the existing 1: 50 000 data (Ahmat, 1986) and provided new zone nomenclature for the WIC and adjacent gabbroic and granitic intrusions (Ivanic, 2011; 2012a,b; 2014; Zibra et al., 2013). These map sheets provide five cross-sections constrained from surface observations (Fig. 4). From this mapping and the new gravity data, with preliminary 2D profile modelling, it was concluded that the WIC was approximately 6 km thick, broadly concentrically layered and bowl shaped with more steeply dipping igneous layering at the margins (Ivanic et al., 2010, 2014; Ivanic, 2014). This is deeper than the estimates of Ahmat (1986) and allow for a larger proportion of ultramafic rocks at the base of the complex.

Additional support for this depth came from the results of three seismic reflection lines. In 2010, seismic lines were planned in order to traverse particular parts of the WIC utilizing existing roads and tracks to provide sufficient data for a 3D seismic interpretation of the complex (Fig. 4). This goal was greatly enhanced by the inclusion of a third line 10GA-YU3 to provide an east–west cross-section of the WIC, supplementing 10GA-YU1 and 10GA-YU2 which both have terminations within the complex. These transects in the vicinity of the WIC had four particular foci: (1) to image across what was thought to be some of the deepest parts of the complex as seen in gravity data; (2) to image across the SDZ and provide evidence for the mechanism of emplacement of rocks to the west of this zone; (3) to image and trace the extent of economically significant magnetitite horizons of the upper zone of the complex; (4) to image across the Challa Shear Zone and the associated metamonzogranite plutons.

The magnetotelluric (MT) conductivity model along the Youanmi seismic lines shows moderate to low conductivity for the ultramafic and lower zones of the complex. This feature appears to be a single, long-wavelength region. Higher conductivity is evident in the surrounding foliated granitic rocks, possibly indicating interconnected conductive minerals in these rocks; for example, within the biotite foliation planes. Short-wavelength anomalies are present in the upper parts of the WIC, corresponding to the magnetite-rich upper zone and roof zone. A 10 km low conductivity feature to the east of the complex on this line is thought to represent late granitic plutons.

Until acquisition of the Youanmi seismic and MT survey, very little attention had been paid to the 3D form of the WIC as a whole. Initial interpretations for each of the three seismic lines in the vicinity of the complex have been presented (Ivanic et al., 2014; Wyche et al., 2014). Here we present updated interpretations of the seismic data and integrate this in 3D with new gravity, and magnetic forward models, and drillcore data along with surface mapping. This modelling is used to tie

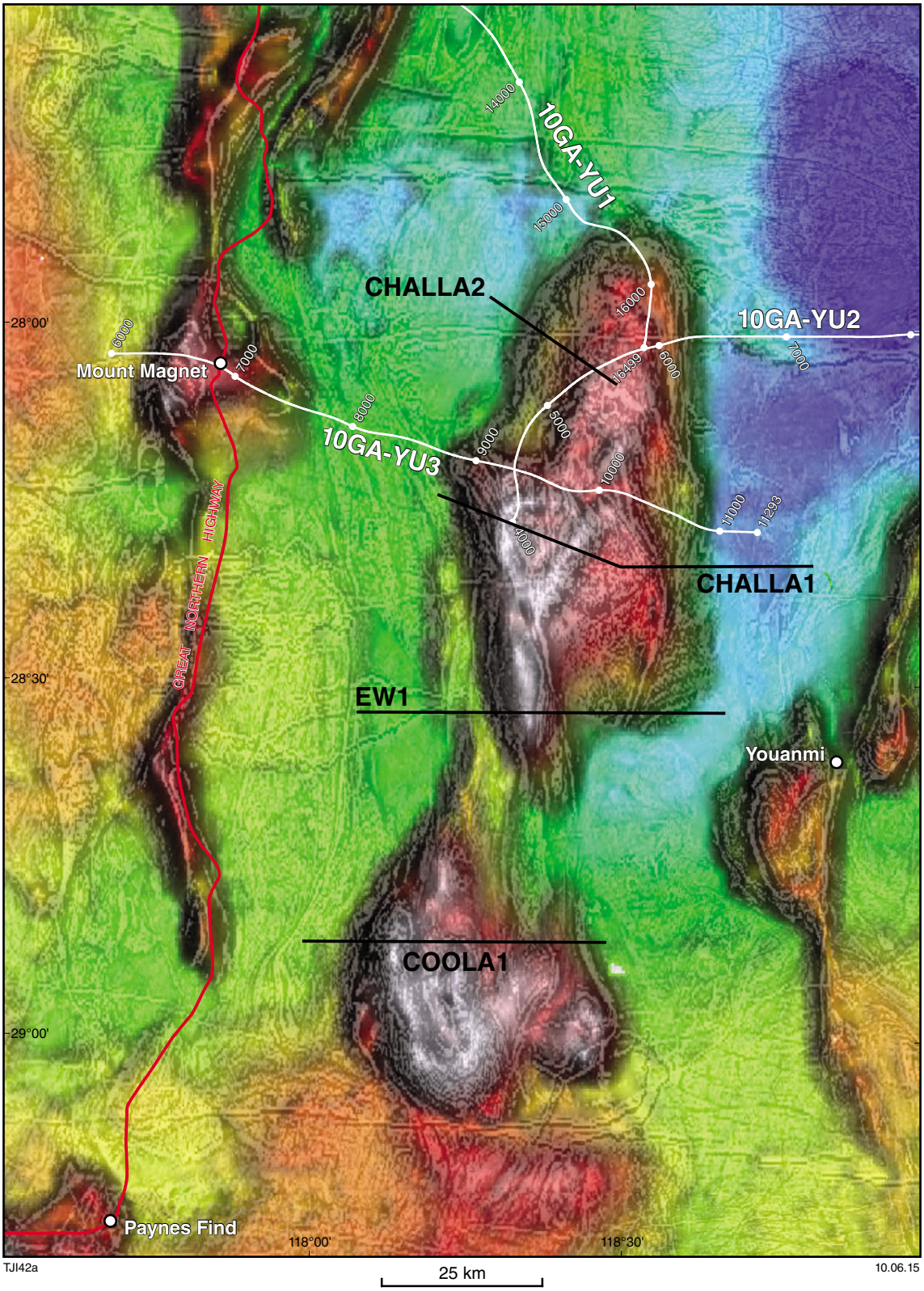

Figure 4. **Location of the Youanmi seismic lines in the vicinity of the Windimurra Igneous Complex (cf. Fig. 1) in relation to combined gravity data (colour) and first vertical derivative magnetic data (shading). In black are the cross-section lines used in the 3D modelling where 'EW1' is the additional line used to further constrain the southern part of the Windimurra Igneous Complex. Challa1, Challa2 and Coola1 are taken from the cross-sections of the 1:100 000 geological map of the same name.**

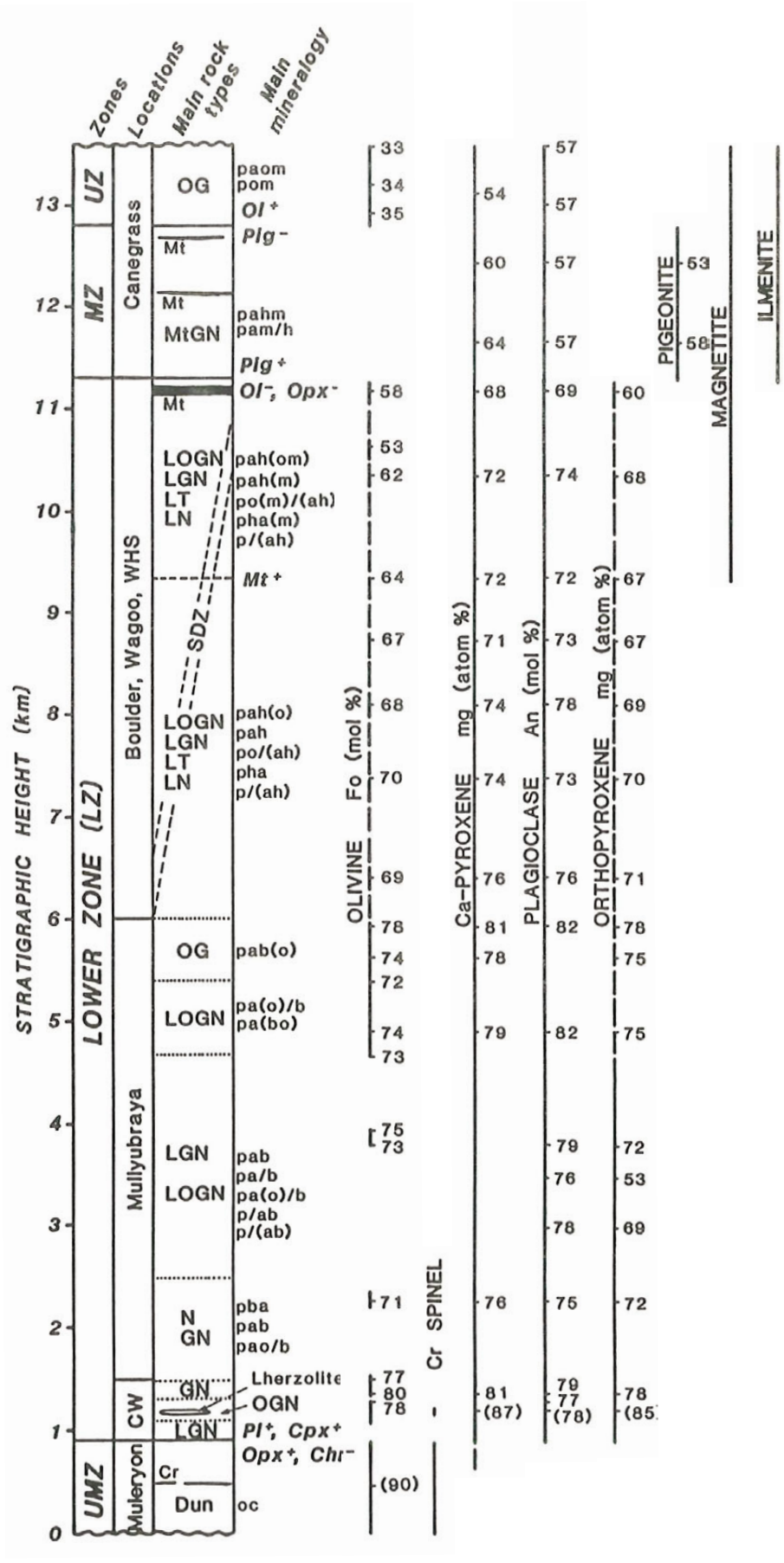
Zones
Locations
Main rock types
Main mineralogy
STRATIGRAPHIC HEIGHT (km)
UMZ
MZ
UZ
LOWER ZONE (LZ)
Muleryon
CW
Mullyubraya
Boulder, Wagoo, WHS
Canegrass
Dun
Cr
GN
LGN
N
GN
LOGN
LGN
OG
LT
LN
Mt
MtGN
SDZ
oc
pab(o)
pa(o)/b
pa(bo)
pab
pa/b
pa(o)/b
p/ab
p/(ab)
pba
pab
pao/b
Lherzolite
OGN
Pl+, Cpx+
Opx+, Chr−
Ol+
Plg−
pahm
pam/h
Plg+
Ol−, Opx−
pah(om)
pah(m)
po(m)/(ah)
pha(m)
p/(ah)
Mt+
pah(o)
pah
po/(ah)
pha
p/(ah)
OLIVINE Fo (mol %)
Cr SPINEL
Ca-PYROXENE mg (atom %)
PLAGIOCLASE An (mol %)
ORTHOPYROXENE mg (atom %)
PIGEONITE
MAGNETITE
ILMENITE
TJI65
10.06.15

Figure 5. (left) Previous interpretation by Ahmat (1986) of the igneous stratigraphy of the Windimurra Igneous Complex showing from left to right: perpendicular stratigraphic height, zone nomenclature, traverse locations, lithologies, textures and the chemostratigraphy of cumulus (solid lines) and intercumulus (dashed lines) phases. Note the diagonal dashed lines representing the Shephards Discordant Zone; however, a clear interpretation for this was lacking. Details of lithological and other acronyms are available in Ahmat (1986).

surface observations with seismic constraints and to test the validity of current interpretations of the form of the complex; in particular, the form and relationships of the more controversial units: the Kantie Murdana Volcanics Member, the SDZ and the ultramafic zone. A variety of geometries of the various components of the complex were assessed using forward and inverse 3D modelling of gravity and magnetic data.

Utilizing these geometric constraints, inferences are made concerning the large-scale magmatic process history for the emplacement of the WIC. In terms of broad layering geometry, we show that the complex can be divided into two discrete bodies: a lower eastern lobe and an upper western lobe with a combined thickness of 11 km. Most significantly, we show that there is a voluminous ultramafic zone that likely underlies the entire complex, which is a potential target for mineral exploration.

Igneous stratigraphy

Understanding the stratigraphic relations of the various zones of the complex is essential for reconstructing its geometry. This stratigraphy represents the primary magmatic control on the igneous sequence onto which are superimposed crosscutting and deformative features (see next section). Furthermore, an appreciation of the variation in the lithologies within these zones allows for a realistic representation of the complicated density and magnetic structure.

The stratigraphy of the WIC (Fig. 6) is comparable in composition to many other large layered mafic–ultramafic intrusions such as the Bushveld Complex (Cawthorn and Walraven, 1998) and others in the Youanmi Terrane. For example the Youanmi, Atley, Barrambie, Lady Alma, and Igneous Complexes are noted to range from 3 to 5 km in thickness (Fig. 6) and possess distinctive magnetitite units in their upper zones. Notably, the Narndee and Gnanagooragoo Igneous Complexes lack these and are not assigned to the same suite as the WIC.

The cumulative thickness of the exposed layers of gabbroic and ultramafic rocks in the WIC is 13 km; however, they exhibit significant lateral aggradation or offlap geometry (Fig. 5; Ahmat, 1986). Thus, this geometry yields a true thickness estimate of about 6 km (Ivanic et al., 2010) as derived from surface constraints (Fig. 6). This is approaching that of the 8.1 km thick Bushveld Complex.

In summary, the complex is divided into eight parts (see Fig. 2):

1. A doleritic border zone (equivalent to the 'Border Group' of Ahmat, 1986). This is typically 100 m thick and occurs along the boundary between sheared supracrustal rocks and the lower zone gabbros. This zone is thought to represent the chilled primary magma, although it is typically recrystallized at amphibolite facies conditions. Examples of granulite facies contact metamorphism of pelitic xenoliths and wall rocks (likely supracrustal rocks of the Norie Group) are preserved in a few locations at the margins of the complex.

2. The ultramafic zone is only exposed in the small outcrops close to Muleryon Hill adjacent to the Challa Shear Zone as a lens detached from the main body of the WIC. It is characterized by abundant peridotite with common accessory-disseminated chromite.

3. The lower zone hosts olivine-rich gabbros and gabbronorites which grade upwards into more leucocratic gabbroic rocks, typically without oxides. These rocks are modally layered on a centimetre-to-metre scale and the rock types are repeated on a 200 m vertical scale. Several kilometres of lower zone are apparently repeated in the western lobe, west of the SDZ.

4. The middle zone is composed of troctolitic rocks with intercumulus magnetite, which are layered in a way similar to the lower zone. This zone appears to be repeated in the western lobe, west of the SDZ.

5. The upper zone is marked by the incoming of vast thicknesses of cumulus magnetite and the disappearance of Mg-olivine (Fig. 5). Within a few hundred metres of the base of the upper zone, Fe-olivine appears as a cumulus phase with magnetite. The majority of rocks in this zone are composed of magnetite-bearing leuconorite and anorthosite, with magnetitite locally abundant. The upper zone of the eastern lobe is truncated by the SDZ, whereas the upper zone of the western lobe appears to have intruded as a single pulse that scoured down into the cumulates of the middle zone of the western lobe (Nebel et al., 2013b). This zone is thicker and apparently more developed in the western lobe; however, it is likely that much of the upper zone of the eastern lobe is not exposed. There are several economic vanadium deposits hosted within the magnetitites of the upper zone (Fig. 3).

6. The Corner Well Gabbro is a late phase of peridotitic-gabbroic pipes, 0.3–2 km in diameter, which have been observed to intrude into the middle and lower zones of the western lobe of the complex (and possibly the lower zone of the eastern lobe). This phase may be consanguineous with the magmas responsible for the main lobes of the WIC; however, geochemical evidence is not conclusive.

7. The roof zone of the WIC comprises kilometre-scale tabular plutons of unlayered dolerite and porphyritic

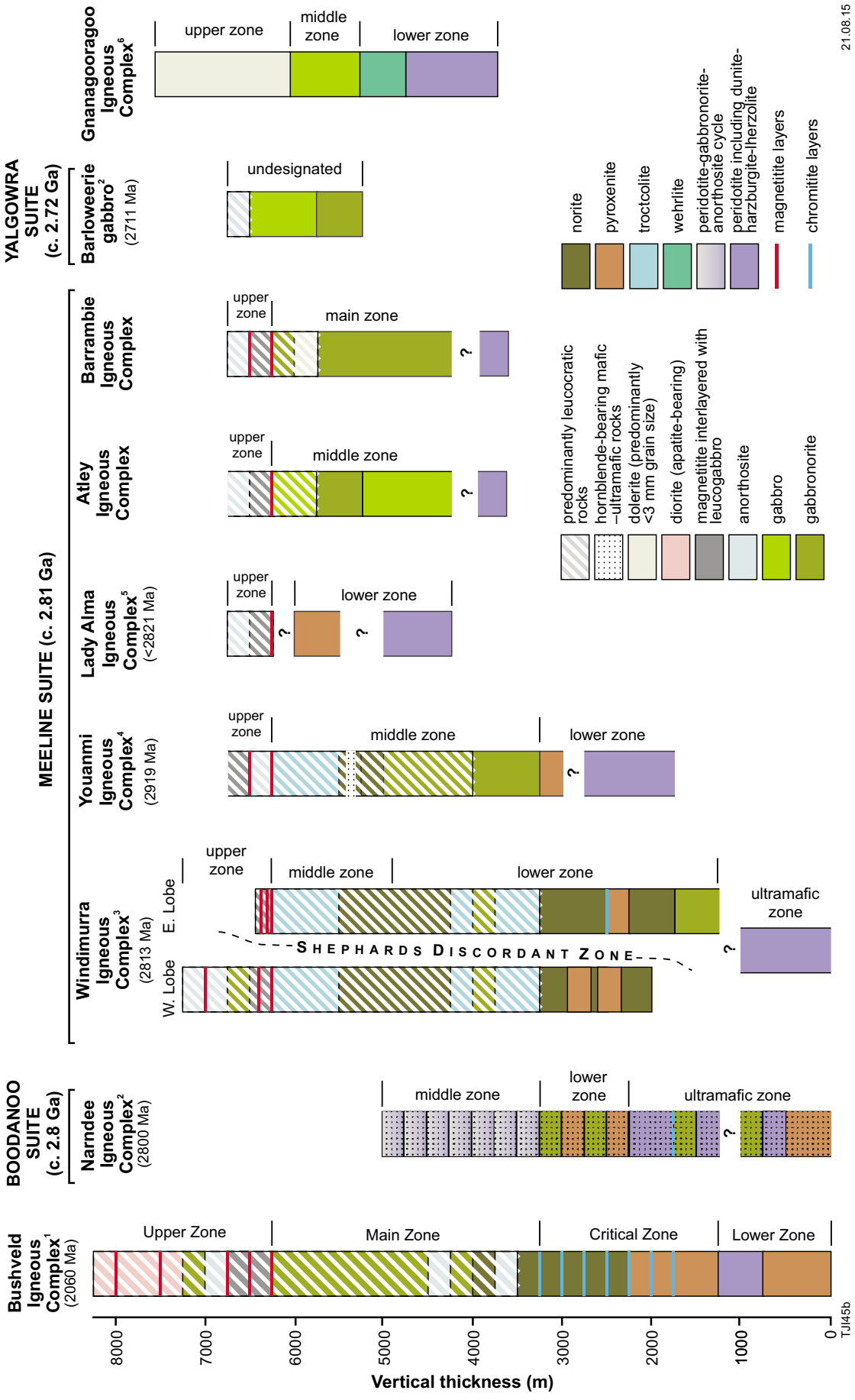

Figure 6. Comparative igneous stratigraphic columns (adapted from Ivanic et al. 2010) for layered igneous complexes of the Youanmi Terrane, compared with the Bushveld Igneous Complex. Simplified stratigraphy is aligned with occurrence of the lowermost upper zone, typically associated with thick magnetitite horizons in the Meeline Suite. Note the lobe and zone interpretation from Ivanic et al. (2014) which shows the repetition within the east and west lobes of the Windimurra Igneous Complex. Also note the chromitite horizons in comparison to the critical zone of the Bushveld Igneous Complex. Notes: [1]adapted from Cawthorn and Walraven (1998); [2]zone nomenclature adapted from Scowen (1991); [3]age from Ivanic et al. (2010); [4]age from Gill (2011), zone interpretation from Ivanic (2014); [5]Wang (1998); [6]Ivanic (2009), zones adapted from (Parks, 1998)

dolerite and gabbro. The basal contact with layered gabbros of the lower zone is not exposed, but its upper contact locally has spinifex-textured gabbros in direct contact with rhyolites of the c. 2813 Ma Kantie Murdana Volcanics Member. According to aeromagnetic data, the roof zone also appears to truncate layered rocks on either side of the SDZ. This zone is interpreted to represent a final phase of shallow-level mafic plutonism whose upper contact chilled against and intruded into overlying rocks, separating them from the layered sequence below. The magma may not have been consanguineous with other parts of the WIC. Immediately overlying the roof zone are tonalitic rocks of the c. 2813 Ma Mount Kenneth Suite and 5–50 m scale apophyses of roof zone dolerite intrudes into these and the Kantie Murdana Volcanics Member.

8. Unassigned units of the complex in several locations along the Challa Shear Zone are detached from any known stratigraphy and are not of distinctive composition, most units being metagabbros with variable preservation of igneous textures. Knowledge of these units is also poor because the outcrop is minor (Ivanic, 2011) due to the proximity of the Challa salt lake system. They include: Boodanoo Hill area, Watsons Well area, West Challa area, Moolyawarda Hill area, and the North Bore area (east of the Challa Shear Zone) as mentioned in Bunting (2004).

In addition to the eight parts described above, there are several other components which may be attributed to the complex:

a) A significant ultramafic zone directly underlying the lower zone and not exposed at the surface. This was postulated to account for the excess in leucocratic rocks in the exposed complex as a whole (Ivanic et al., 2010). This unit might include a preserved feeder system.

b) Amphibolitic xenoliths up to 300 m in size within metagranitic rocks in a c. 50 km radius around the complex.

c) It is possible that either the Youanmi or the Atley Igneous Complex (Fig. 1) or both could have been part of the WIC as separate 'lobes', now separated by a 12–32 km width of granitic plutons.

d) Significant thicknesses of portions of the complex may have been lost through erosion.

e) An area of high-gravity response to the south of the Narndee Igneous Complex (Fig. 4), approximately 30 x 30 km, may be a sinistrally displaced part of the western lobe of the WIC (i.e. with c. 80 km displacement).

Discordance

A discordant zone within a layered magmatic body is a plane of 'unconformity' between two layered packages whereby one package either onlaps onto or truncates the layers of the underlying package. This is differentiated from a fault or shear zone because there is little or no deformation associated owing to the inferred liquid-present accommodation of any movements.

The SDZ, which is at least 20 km long, represents a significant break in the igneous stratigraphy (several kilometres, see Fig. 6). However, the precise origin of this feature is still not fully understood since arguments for both structural and magmatic processes have been postulated (Ahmat, 1986; Bunting, 2004). It is clear that the SDZ separates the complex into two main parts: an eastern lobe and an apparently transgressive western lobe, both of which contain a lower, middle and upper zone of a similar nature. However, what becomes of this discordant relationship underneath the Kantie Murdana Volcanics Member and to the west is not clear.

Another significant discordant feature is located at the base of the upper zone magnetitites in the vicinity of the Canegrass vanadium/iron resource in the western lobe of the complex (diamond drillholes 1–4, Fig. 2). Here, the upper zone has an undulating basal contact which appears to have scoured into underlying middle zone rocks, creating a 'base breccia' identified in drillcore (Nebel et al., 2010). The relationship of this feature to the SDZ is not clear from surface observations.

Contact relations and structural overprint

There are many unknowns remaining concerning the contact relationships of the WIC and younger structures in the area. These are mainly at depth, but also near surface where many key contacts and faults are under cover. 3D modelling presented here aims to clarify many of these issues and what follows is a description of the state of our knowledge prior to the modelling in this study.

Little is known about the basal contact of the WIC as it is unexposed. It is inferred from seismic data to be predominantly intruded by later granitic rocks (see below; Ivanic et al., 2014). However, at the time of intrusion of the complex, the substrate was likely c. 3 Ga basement gneisses of the Youanmi Terrane. A chilled border zone (<500 m thick) and an ultramafic cumulate belonging to an ultramafic zone of the WIC was likely in contact with this host rock.

The WIC is in sheared contact with host rocks of the Norie Group in several places around its northwestern, northern and eastern sides. In these areas, some xenoliths of supracrustal country rocks are preserved, which suggest that the complex intruded into Norie Group host rocks. The border zone is postulated to have formed by chilling of magma along these contacts (Ahmat, 1986) immediately prior to the accumulation of the layered series of zones.

The roof zone, as described above, is thought to represent a complex zone of late-stage intrusive gabbroic rocks which were chilled locally at their upper contact with the Kantie Murdana Volcanics Member. Contact metamorphism is thought to be responsible for recrystallization of rhyolitic rocks of this member. The

Mount Kenneth Suite of granodioritic plutons is also thought to be associated with the rhyolitic volcanics (Ivanic, 2012a) and a few of these are mapped at the surface adjacent to the Kantie Murdana Volcanics Member.

Metamonzogranites (c. 2700 Ma Big Bell and the c. 2680 Ma Tuckanarra Suites) are observed to be in sheared contact with the lower, middle, upper and border zones of the complex, where it is evident that they truncate many of the macroscopic igneous layers on aeromagnetic maps. These layers are locally deformed into parallelism with shear zones and metamonzogranites. Bald Rock Supersuite granites intrude across the southern part of the complex, where they are interpreted to have cut across sheared layering of the complex (Ivanic, 2011; 2012b; 2014). In addition, Wogala Suite Li-rich pegmatites (belonging to the Bald Rock Supersuite) crosscut layers of the lower zone of the complex. According to seismic observations (Ivanic et al., 2014), it is likely that these four suites of granitic rocks intrude into the basal contact of the complex at considerable depth, possibly obscuring much of the original basal contact with basement gneisses.

There are several shear zones observed around the western, northern and eastern parts of the complex where metagranitic rocks are typically in contact with sheared supracrustal rocks (Fig. 2). The Yarloo Shear Zone deforms metagranitic rocks at the northwest of the complex and appears from aeromagnetic data to be crosscut in the south by the Challa Shear Zone (Ivanic, 2012a). The Challa Shear Zone is the most significant shear zone to affect the WIC since it is responsible for transportation of lenses of the complex up to (and possibly further than) 30 km away from the core of the complex (apparently on a large scale, with a sinestral sense). However, there are locally abundant dextral shear sense indicators observed along this shear zone and hence it is likely that it has subsequently been reactivated in a dextral sense at c. 2680 Ma, the age of syn-tectonic Tuckanarra Suite plutons in the area.

The Wyemandoo Shear Zone in the southeast of the complex displaces igneous layering and the SDZ. This shear zone juxtaposes lenses of metamorphosed supracrustal rocks and amphibolitized gabbro lenses, with less sheared gabbroic rocks of the complex on either side. There is also another minor shear zone with similar characteristics in the northwestern part of the complex (the Mingyngura Hill area Fig. 2; Ivanic, 2012a), which brings supracrustal rocks into contact with the internal parts of the complex.

Tight folding on a 500 m scale is evident in the Kantie Murdana Volcanics Member and also in supracrustal rocks immediately to the north of the complex. These locations are both in the region of tightest curvature in the large-scale layering of the WIC. Axial planes are typically steep and northerly trending with an associated, moderately north-plunging, lineation. This is consistent with an overall east–west shortening along a north–south axis and moderate downwarping along a north-plunging axis. If the complex is taken as an originally circular form which has become an ovoid strain ellipse, this would indicate ~2:1 east–west shortening. A synformal axis of hinge formation is indicated on the Windimurra and Challa 1:100 000 map sheets (Ivanic, 2012a, b).

Abundant, north–south trending, steeply dipping brittle faults in the central part of the complex offset contacts between the various zones described (Fig. 2). Although the displacement cannot be measured directly, the mechanism is consistent with normal faulting (including antithetic faults) and 50–500 m of offset based on map patterns. A set of northeasterly trending brittle faults in the south of the main body of the complex dextrally offset the Wyemandoo Shear Zone with strike-slip displacement of up to 1000 m based on map patterns. Another set of brittle faults in the northeastern part of the complex trends northwest and dextrally offsets igneous layering, the border zone and lateral shear zones around the complex by between 50 and 3000 m.

Input data for the 3D model

Good geophysical data coverage in the area around the WIC has enabled this study to advance the limited understanding of the complex derived from surface geological observations and to augment conceptions about the vertical extent and original architecture of the complex. The construction of the 3D model was intended specifically to be simplified (i.e. incorporating only first order structures and lithological zones), utilizing only orientation and contact data from well understood regions of outcrop and in the seismic data, validated against gravity data. Moreover, a low-resolution model is considered suitable given that there is still a high degree of uncertainty about the location of several key components of the complex. The effective resolution of the 3D map is coarse; it is essentially a 1:1 000 000 scale product with a 1 km resolution.

Although providing limitations in terms of detail, this methodology has enabled a geological approach to dominate the study. Emphasis is given initially to high-quality geological map data with subsequent constraints imposed by geophysical data. The coarse resolution has allowed a geological focus on fundamental model geometries, which can be tested through forward geophysical modelling. One advantage of this approach is more flexibility, compared with an 'over-constrained' or highly complex model. The result of this methodology is to provide first order information on the likely form of the various components of the complex, which has enabled some speculation as to the magmatic processes necessary to explain this geometry.

Geophysical data

Grids of magnetics and gravity were sourced from the Western Australian state geophysical compilations gridded at ~400 m for gravity and 80 m for magnetic data. The magnetic data is in units of nanotesla (nT) RTP (reduced to pole). The gravity data was converted from gravity units (μms^{-2}) to milligals (mgals). A first order trend was removed from both gravity and aeromagnetic surveys to remove regional effects that could not be accounted for in the 3D model. In order to counter the effect of bodies around WIC, the forward modelling and inversion were

conducted on a smaller volume than for the whole 3D model. The magnetic data was upward continued by 1000 m to attenuate very short wavelengths that could not be accommodated with the voxel element size used for the inversion. Grids were then imported into the GeoModeller project. MT data was not utilized in this study.

The region of outcrop of the WIC has a substantially higher gravity response than surrounding metagranitic rocks (Fig. 2) as would be expected for more ferromagnesian plutonic rocks. Superimposed on this, distinct high-gravity features occur within the WIC, which are focused in its central parts but with a bias towards the southwestern sheared margin of the western lobe. Magnetic data provides excellent trend lines of igneous layering features (Fig. 2). In the lower zone olivine-rich cumulates create thin linear trends of high magnetic response, interpreted to represent metamorphism to magnetite + serpentine. In the middle and upper zones, the incoming primary magnetite translates to thick and high magnitude magnetic highs. Faults may also be interpreted based on the offsets of these features. Regions showing distinctly low magnetic response in the south of the WIC and in the northwest are thought to be caused by magnetic remanence effects.

Physical properties

Rock property data (density and magnetic susceptibility) were compiled from several sources (Tables 1–3) for the purpose of estimating average rock volume values for the various modelled packages:

1. Values used for previous gravity modelling (Ahmat, 1986; Table 1)
2. Maximus Resources downhole geophysics data from two of four drillholes from the Canegrass prospect (Fig. 2, Table 2)
3. GSWA samples analysed at the Australian National University (Table 3)
4. Values used in the gravity forward modelling of the seismic line (Gessner et al., 2013).

The magnetic susceptibilities and densities of each package are shown in Table 1 with expected standard deviations shown for bimodal and unimodal distributions. Bimodal distributions were defined for units that are expected to be distinctly heterogeneously layered in terms of their density or magnetic susceptibility. The basal layer, the mantle (unit 1, Table 1), is deemed not to have any magnetic effect on aeromagnetic data.

Seismic processing

Details of seismic acquisition and processing for the WIC including specific observations on its seismic characteristics, were presented in Jones et al., 2012. Seismic processing obtains seismic velocity in two ways: bedrock velocity as a byproduct of refraction statics analysis, and interval velocity as a derivative of stacking velocity analysis. High bedrock and interval velocities mostly exceeding 6250 ms^{-1} (and up to approximately 6500 ms^{-1} locally,) correspond with the location of the WIC (Jones et al., 2012). Seismic attenuation is low, resulting in high-frequency reflections with good resolution down to the base of the complex, thus facilitating detailed interpretation. Full details of acquisition and processing are described in Costelloe and Jones, 2014.

Several workshops were held in 2013 in order to make initial geological interpretations along all parts of the Youanmi seismic lines (Wyche et al., 2014; see Acknowledgements). Following this, we present a summary of the interpretation in the vicinity of the WIC which includes additional details. Once finalized, the interpreted cross-sections along the seismic lines were adapted and imported for use with 3D modelling software (Fig. 7 showing interpreted sections).

GeoModeller

The software used to build the 3D model (Model 3) was GeoModeller by Intrepid Geophysics (Melbourne). GeoModeller is a 3D geological modelling tool used for building complex, steady-state, 3D geology models and for performing forward and inverse geophysical modelling directly from solid 3D geology. Later these shapes were translated to GOCAD for presentation purposes.

The first consideration for the 3D model was the extent of the bounding box volume. We selected an area which encompassed the YIC and the Narndee Igneous Complex in case they were to be modelled at a later stage (Table 4). The depth was defined at 50 km (i.e. down to below the Moho), as the Moho was well defined on the Youanmi seismic lines and the height above the surface, sufficient to model a substantial thickness of displaced stratigraphy.

Second, we considered the resolution of observations to incorporate for the purpose of fulfilling the objectives of this study. Hence, the resolution of one kilometre-scale was chosen (i.e. a discretization value of 1000 m), so that we could model features on the order of the scale of the gravity observations (2.5 km separation between observations) and we would not over-define the model. The complexity of the brittle faulting (all estimated at <1 km displacement) could be avoided without significant disruption of gravity modelling.

Table 1. Summary of rock properties used in Ahmat (1986)

Lithology	*Average density (g/cm^3)*
Generic 'Windimurra Gabbroid'	2.89
Shephards Discordant Zone	3.10
'Middle Zone – Upper Zone'	3.15
Felsic schists	2.70
Mafic intrusives, Kantie Murdana Volcanics Member	3.05
'Granitoid'	2.65

Table 2. Summary of downhole geophysics results from MNDD002 and MNDD004 form the Canegrass prospect. Note that high average densities and standard deviations here are expected given the high abundance of magnetite and fayalitic olivine in many of the intersected lithologies. Their interlayering with anorthositic rocks is interpreted to have yielded high standard deviations.

Region	*Average magnetic susceptibility (S.I units)*	*Standard deviation*	*Average density (g/cm^3)*	*Standard deviation*
Drillhole MNDD004	0.30	0.27	3.44	0.36
Drillhole MNDD002	0.50	0.28	4.13	0.54
Upper zone sheet (from MNDD002 <150m)	0.57	0.26	4.19	0.65
Middle zone average (from lower half MNDD004)	0.27	0.16	3.52	0.19

Table 3. Summary of rock density determinations for GSWA samples

GSWA sample no.	*Lithology*	*Rock unit*	*Density (g/cm^3)*
178101	granitic rock	Tuckanarra Suite	2.65
185922	gabbro	Yalgowra Suite	3.06
178197	monzogranite	Jungar Suite	2.64
198220	monzogranite	Walganna Suite	2.65
198209	psammitic schist	Norie Group	2.66
198210	foliated metagranite	Jungar Suite	2.66
198132	sheared gabbro	Unassigned amphibolite	2.92

In addition, the known complexity of the repetitive modal igneous layering of the WIC could not be accurately estimated far beneath the surface. Hence it would be averaged at this scale in terms of geometry and physical properties.

With the region and resolution defined in this way, the appropriate means to divide the WIC into amenable rock volume packages would be to subdivide the complex into several components based broadly upon the zone nomenclature (above). External units to the WIC would also be readily modelled at this scale, i.e. the large-scale crustal features such as granites, basement rocks and associated major shear zones adjacent to the WIC.

Features that were too small to model here are as follows: (1) brittle faulting and smaller shear zone geometry; (2) the border zone; (3) the Corner Well Gabbro pipes; (4) separation of the roof zone gabbros from the felsic volcanics and banded iron-formation of the Kantie Murdana Volcanics Member and Mount Kenneth Suite granitic rocks; (5) individual megacyclic units as even the largest of these are <500 m thick; (6) regions of the upper zone rich in magnetitite as these are interlayered with a variety of lithologies on a metre scale; (7) the Wyemandoo Shear Zone was considered too thin to include in this model; (8) Proterozoic sills and dykes. These are too thin at <100 m and also likely have similar geophysical properties to the gabbroic rocks of the WIC; (9) the regolith (maximum thickness approximately 100 m); (10) the topography (variation <100 m).

A compilation of depth-converted seismic sections and existing cross-sections from 1: 100 000-scale mapping was imported and georeferenced in GeoModeller. The surface topography was added as a flat horizon at 450 m elevation ('Windi_SRTM_Elevation'). A simplified interpreted bedrock map was added to this topographic horizon with relevant structural data ('rec2015_12_fig2_prelim' in 3D geomodel).

Table 4. Maximum and minimum values in the coordinate system MGA zone 50 for the modelled volume in metres

	Minimum	*Maximum*	*Length*
Easting	555 000	705 000	150 km
Northing	6 750 000	6 950 000	200 km
Depth	-50 000	10 000	60 km

Construction of the 3D model

Map data was digitized onto the surface section in GeoModeller according to the boundaries of the rock packages defined. Structural data for igneous layering was added to the model where known, and was as widely distributed as possible. Faults were drawn and their structural orientation data were added for these where known. Following this, boundaries and orientation data were entered from the seismic lines and then from cross-sections taken from the 1:100 000 maps.

This geological data were entered iteratively from simple, large-scale features initially, with more intricate detail added later and as deemed necessary for geophysical modelling. Initially, all shear zones and faults were ignored in order to assess the potential size of the complex prior to deformation (Model 1). Subsequently, the Challa Shear Zone was incorporated along with shear zones around the northern part of the complex (Model 2). The smaller-scale Wyemandoo Shear Zone and north-south-trending brittle faults were not modelled given the relatively coarse resolution of this model.

The interpreted geometries from the three seismic lines 10GA-YU1, 10GA-YU2 and 10GA-YU3 (see results section) were input into the model. A list of cross-sections utilized in the 3D model is given below (see also Fig. 4):

1. 'YU1-curve' — Southern 10 km of seismic line 10GA-YU1
2. 'YU2-curve' — Western 30 km of 10GA-YU2
3. 'YU3-curve' — Eastern 40 km of 10GA-YU3
4. 'COOLA1' — 1:100 000 map sheet cross-section: Coolamaninu E-W
5. 'CHALLA1' — 1:100 000 map sheet cross-sections: Challa (S) linked to Windimurra E-W
6. 'CHALLA2' — 1:100 000 map sheet cross-section: Challa (N)
7. 'EW1' — A supplementary cross-section for extra control on the model geometry at the southern tip of the complex
8. Surface section ('Windi_SRTM_Elevation' in 3D geomodel)

Lithological packages and shear zones

The simplified stratigraphy used is shown in Table 5 using 'base of' unit definition (i.e. not 'top of'). Within the WIC the main components identified from map and seismic data were the hidden ultramafic zone, the lower zone of the eastern lobe, the middle and upper zones of the eastern lobe (grouped because the upper zone is locally <1 km thick), the lower and middle zones of the western lobe, the upper zone of the western lobe, and the roof zone merged with the Kantie Murdana Volcanics Member.

In the seismic lines, a significant distinction is apparent between the middle crust and the upper crust at the 4–5s interval. Therefore the 'Litho' package (Table 5) is equivalent to the 'Yarraquin Seismic Province' identified in (Korsch et al., 2014) consisting of high-amplitude, parallel, east-dipping reflectors. This package is deemed to have a higher density than the upper crustal 'basement granites' owing to higher pressure and higher Fe-Mg content of less evolved rocks.

Table 6 shows the magnetic and density values used for each unit. These are adapted from values in Tables 1–3. The fault matrix for the three major shear zones in the model is shown in Table 7 where the Challa Shear Zone is the latest feature, crosscutting the older shear zones (the Yalgar and 'eastern' shear zones). The faults were constrained to cut all stratigraphy except for 'post-tectonic granites', 'lithosphere' and 'lithospheric mantle'.

Table 5. Modelled stratigraphic column describing the features merged

Unit order and codename	*Unit name*	*Comments*
V01_BaldRockSupersuite	Post-tectonic granites	≡ Bald Rock Supersuite
V02_KantieMV_RoofZone	Roof zone and Kantie Murdana Volcanics Member	Each are <1 km thick on their own so have to be merged
V03_UpperMiddleZonesWest	Upper and middle zones of the western lobe	Upper zone treated as a single sheet (single pulse; Nebel et al., 2013b) plus similar lithologies of the middle zone
V04_LowerZoneWest	Lower and middle zones of the western lobe	Units immediately above the Shephards Discordant Zone
V05_UpperMiddleZonesEast	Middle and upper zones of the eastern lobe	Grouped because the upper zone is locally <1 km thick
V06_LowerZoneEast	Lower zone of the eastern lobe	Large thick zone
V07_UltramaficZone	Ultramafic zone	Large thick zone
V08_Metagranites_Basement	Pre- and syn-tectonic granitoids, upper crust basement	Mainly Tuckanarra, Big Bell, and Mount Kenneth suites; may include >2900 Ma basement
V09_YarraquinSeismicProvince	Mid-lower crustal gneisses	≡ 'Yarraquin Seismic Province' identified in Korsch et al., 2014
LithoMantle	Lithospheric mantle	Tabular layer below the Moho

Results

Interpretation of the seismic lines across the WIC

The interpretations of the seismic data in the vicinity of the WIC are presented in Figure 7 and described below. The interpretations were checked for 3D consistency and boundaries were fixed on multiple seismic line junctions.

General seismic observations

In the vicinity of the WIC, the Moho appears slightly elevated by 0.3 s two-way travel time (TWT, about 1 km), compared to the northern Youanmi Terrane. However, the higher seismic velocities within the WIC are sufficient to explain this difference and hence the Moho may in fact be flat. Apart from this, there are flat and relatively uniform reflections below 9 s TWT (~27 km depth) within the Moho transition zone. Between 3 and 9 s TWT (4 and 9 s TWT on 10GA-YU3, about 12 and 27 km depth), there are a series of strong reflections dipping distinctly ~15° to the east. This is interpreted to be the layered, intermediate middle crust with a strongly listric geometry (i.e. the Yarraquin Seismic Province). There is a distinctive region of this middle crust as shallow as 2.4 s TWT (about 7.2 km) just to the north of the complex (seen in line 10GA-YU1). This region deepens to a more typical level for the Youanmi Terrane of 4 s TWT (~12 km) towards the central and southern parts of the complex (see Plate 3 in Wyche et al., 2014).

In one seismic zone with no distinctive features and low general reflectivity (e.g. 10GA-YU1 CDP15500–16000 at 2–3s TWT), upper crustal granitic rocks are interpreted to overlie the strongly anisotropic middle crust and underlie the WIC. Some of these granitic rocks are interpreted to be in sheared contact with the ultramafic zone at the base of the complex, and attributed to the Tuckanarra and Big Bell suites, as these units can be traced to surface outcrops. Some of these granitic rocks at depth, however, may include older suites (<2813 Ma) which acted as a basement to the complex. Some of these basement granites may belong to the Mount Kenneth Suite which, when exposed at the surface, are typically deformed and interlayered with felsic supracrustal rocks of the Norie Group. In addition, there are several instances where the seismic data show crosscutting granitic plutons of the Bald Rock Supersuite, some of which can be related to surface exposures of the supersuite.

Using information from all of the Youanmi seismic lines, the general form of the WIC is a shallow, funnel-shaped cone, with inward-dipping reflections. The seismic character is twofold with regions of very strongly layered and reflective features, and regions of less strongly reflective, but still layered, features. In each of the seismic lines, these layered features in both seismic regions, typically follow the outer (funnel-shaped) form of the complex as a whole. The upper part of the complex, in contrast, is strongly anisotropic in terms of the mineralogy (and hence, density) of its lithologies and shows some layering complexity visible especially in its central part on 10GA-YU3 (Fig. 7c). This may be partly due to out-of-plane reflections caused by 3D effects, but also some local complexities associated with brittle faulting.

The maximum true thickness of the lower, strongly layered region is 1 s TWT (about 3 km) and the maximum thickness above this is 2.3 s TWT (about 6.9 km), both evident on 10GA-YU3. Therefore a minimum estimate for the maximum true thickness of the complex is 10.5 km. In terms of stratigraphic thickness (that is, in a perpendicular transect of continuous igneous stratigraphic layering in 2D, where layering is not truncated) the maximum thickness obtainable from seismic observations is 3.7 TWT (~11.5 km).

The lowermost region is characterized by strongly layered, high-frequency reflections, whereas, above this, it is seismically less reflective, with more discrete reflective horizons. Strong reflectors in the lowermost region are likely produced by high impedance contrasts in cyclical, modally layered igneous rocks. High impedance contrasts are most likely due to peridotite-gabbro variation as these have distinctly different densities and velocities. More specifically, cumulates of peridotite, chromitite, pyroxenite and gabbro, are likely interlayered on a decametre scale at this level of a mafic–ultramafic intrusion. However, the spacing between major reflectors in this zone is on a 300–500 m scale, which is indicative of the thickness of megacyclical units of an 'ultramafic zone'. For the upper region, the lithology contrast between pyroxenitic and anorthositic layers on a ~300 m vertical scale (as observed at surface) is consistent with the abundance and magnitude of these more discrete reflections, corresponding with lower zone rocks exposed at the surface.

The regions of middle and upper zones on the seismic lines appear similar, owing to the presence of high-density contrasts in the lithologies of these zones (i.e. anorthosite, gabbro, and magnetitite, with the latter much more common in the upper zone). The upper zone appears to be well constrained in the upper seismic region where very flat-lying reflections in 10GA-YU2 and 10GA-YU3 are evident. This is consistent with the dip of layering as observed at the surface. It is also consistent with the interpretation that this layer intruded as a crosscutting sheet into at least the middle zone of the western lobe of the complex and possibly into its lower zone and the various zones of the eastern lobe. This truncation is evident in the 10GA-YU2 and 10GA-YU3 (Fig. 7b,c,e and f).

Each seismic line shows a chaotic, poorly stratified region corresponding with unit 9 (Table 5; interpreted to be the roof zone of the complex and the overlying Kantie Murdana Volcanics Member), which crosscuts all other zones of the complex, again consistent with surface observations. These contacts appear to dip at a shallow angle (<10°).

Table 6. Magnetic susceptibilities and densities for each unit showing standard deviations used for unimodal and bimodal distributions. Parentheses figures are the percentages defined for the proportion of Mode 1 or Mode 2.

	Magnetic susceptibility (SI units)				*Density (g/cm³)*			
Unit	*Mode 1 mean*	*Mode 1 st. dev.*	*Mode 2 mean*	*Mode 2 st. dev.*	*Mode 1 mean*	*Mode 1 st. dev.*	*Mode 2 mean*	*Mode 2 st. dev.*
10	0.005	0.0005			2.60	0.4		
9	0.08	0.008			3.00	0.3		
8	0.12 (66)	0.04	0.06 (34)	0.004	3.10 (40)	0.2	2.80 (60)	0.2
7	0.03 (70)	0.006	0.06 (30)	0.0095	2.70	0.2		
6	0.12 (30)	0.04	0.06 (70)	0.004	3.10 (50)	0.2	2.80 (50)	0.2
5	0.03 (70)	0.006	0.06 (30)	0.0095	2.80	0.2		
4	0.04 (40)	0.01	0.06 (60)	0.02	3.00	0.3		
3	0.01	0.002			2.65	0.1		
2	0.01	0.001			2.67	0.15		
1	0	0			3.00	0.2		

Table 7. Modelled shear zones in the 'fault matrix'

Stops on ➔ / *Fault name*	*F01_ ChallaShearZone*	*F03_ WindiEastShearZone'*	*F02_ YarlooShearZone*
F01_ChallaShearZone	–		
F03_WindiEastShearZone	TRUE	–	TRUE
F02_YarlooShearZone	TRUE		–

Observations from 10GA-YU1 (CDP 15300–16497)

As the line traverses the complex from the north, it progresses up-stratigraphy through the lower zone and, at the southernmost part of the line, it crosses into surface exposures of the Kantie Murdana Volcanics Member (see Fig. 7a,d). This line terminates at CDP5880 of 10GA-YU2.

At CDP15300, the west-dipping Yarloo Shear Zone has been inferred using aeromagnetic interpretation. Exposure is poor in the area, however, and so this feature is not well described. Granitic rocks in the vicinity have a steeply dipping, northerly striking foliation, which strikes at a small angle to the seismic line. Thus, they are expressed only as shallow-dipping reflections on this section. The shear zone is interpreted to be within metagranitic rocks of the c. 2700 Ma Big Bell Suite.

Felsic schists assigned to the Norie Group, Yaloginda Formation, including metasedimentary rocks (A-NOy-md on Fig. 7c), which mantle the WIC, are not reflective but are interpreted to occur in a small wedge immediately to the north of the complex between shear zones. Rocks of this unit are only exposed in a small outcrop (200 x 200 m) north of the complex (Zibra et al., 2013).

Relatively shallow-dipping reflections characterize the lower zone of the complex. Corresponding surface exposures of modally layered gabbroic cumulates are known to have similar dips of 15–30° across this region, which are compatible with these reflections. Towards the southern end of the line (closer to the centre of the complex), these dips shallow to almost horizontal, as shown by the reflections in the lower zone towards the southern limit of the line.

At the northern contact of the WIC on this seismic line, there is an intersection of the complex with a highly reflective and gently north-dipping unit. Features such as this are extensive on this line further north and on 10GA-YU2 and are interpreted as Proterozoic sills of the Warakurna Supersuite (Ivanic et al., 2014). It is inferred that this sill correlates with the Mount Holmes Gabbro sill which outcrops to the east of the WIC and is readily visible in seismic line 10GA-YU2 (easternmost part of Fig. 7b,e). In this instance, it is apparent that the high impedance contrast of the sill within surrounding granitic rocks transitions immediately once within the WIC into an impedance contrast of close to zero. Hence, it appears that the WIC crosscuts the younger sill, whereas the sill is effectively 'seismically truncated' rather than being geologically truncated. This feature is considered to be below the resolution of the 3D model and is therefore not included.

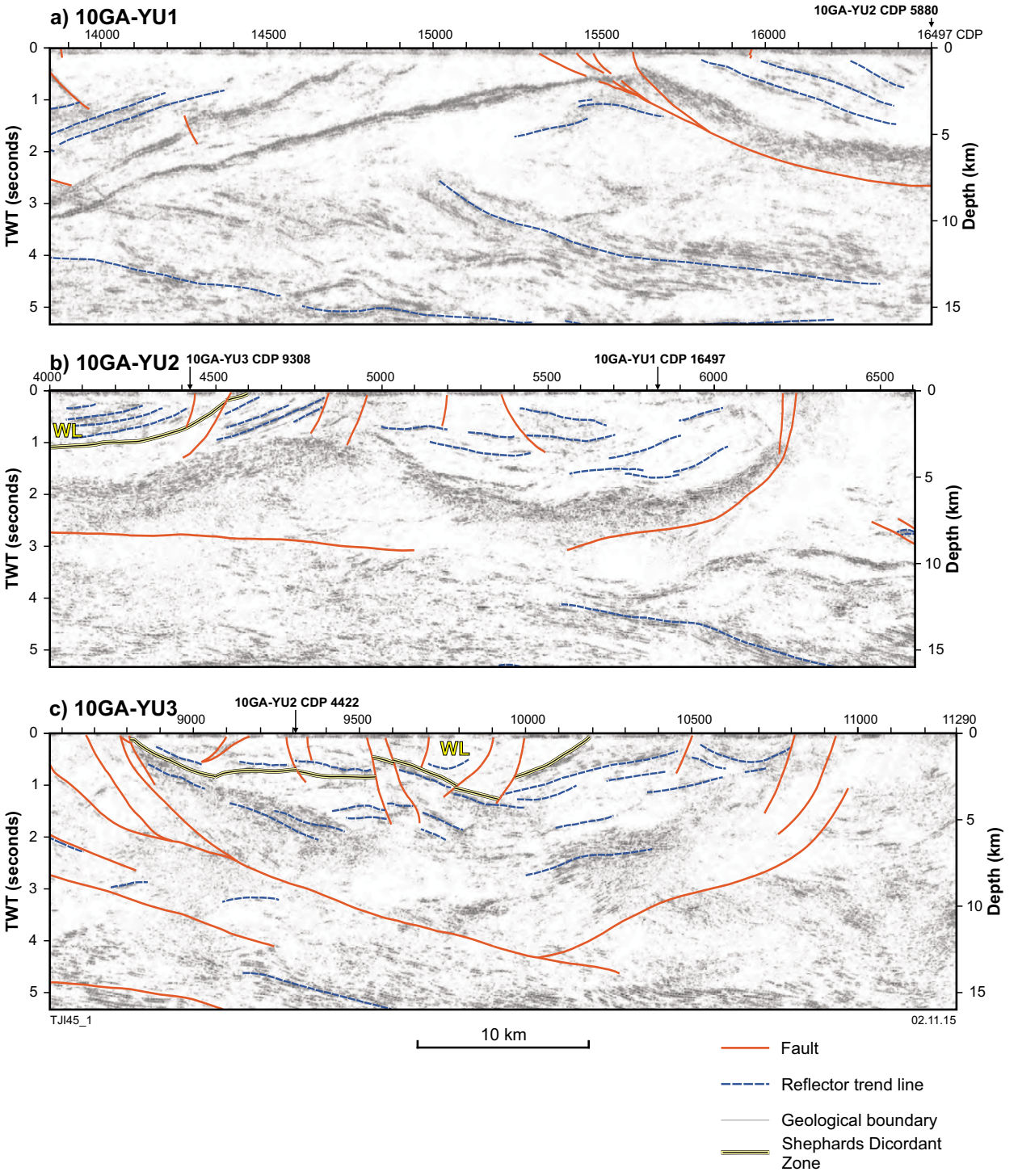

Figure 7. **(a) Migrated seismic data from 10GA-YU1 showing interpreted structural features; (b) migrated seismic data from 10GA-YU2 showing interpreted structural features (note 'WL' = western lobe defined above the Shephards Discordant Zone; (c) migrated seismic data from 10GA-YU3 showing interpreted structural features (note 'WL' = western lobe defined above the SDZ). Interpretation of the seismic lines showing lithologies (GSWA codes from 1:100 000 maps) for (d) 10GA-YU1; (e) 10GA-YU2 and (f) 10GA-YU3.**

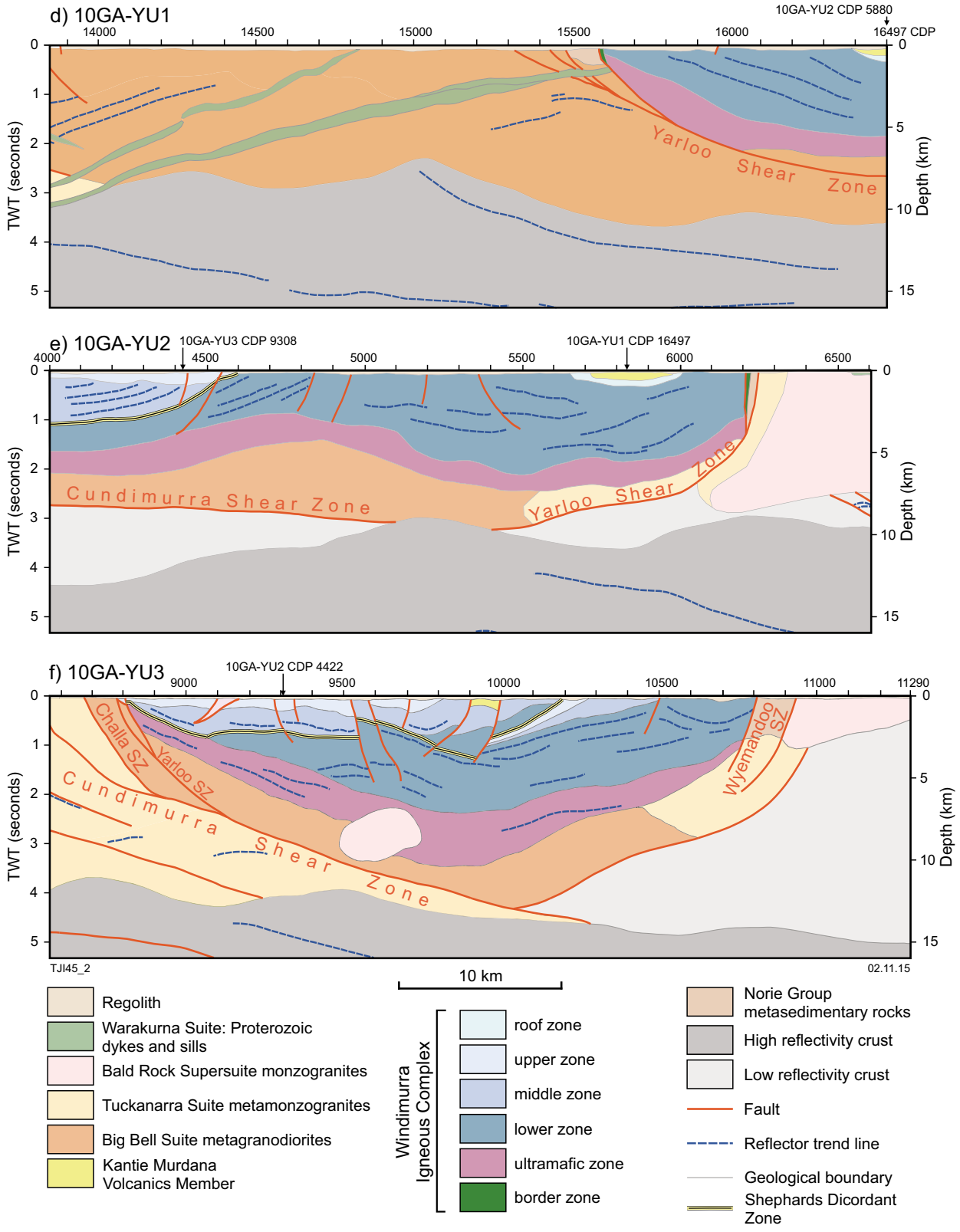

Figure 7. continued

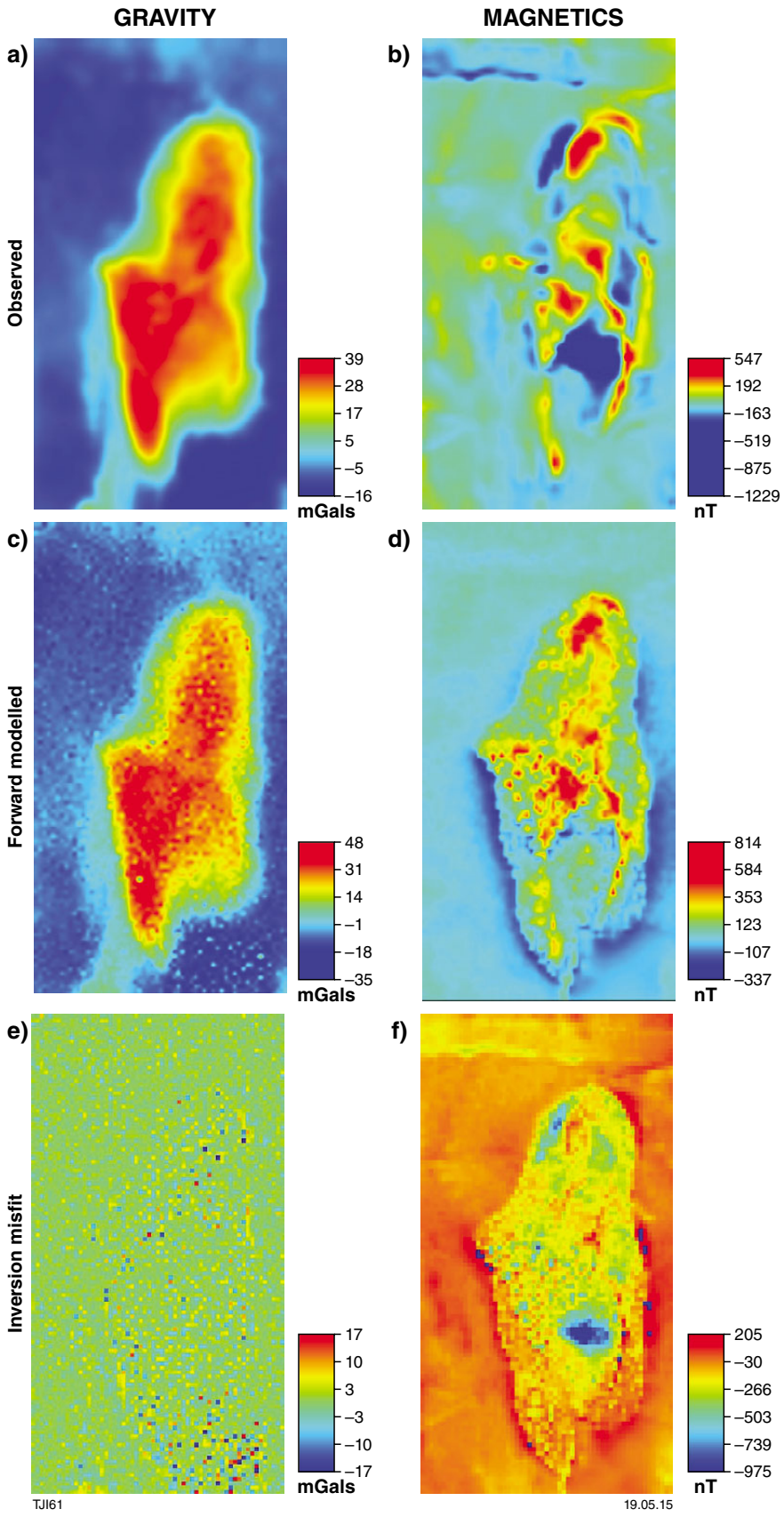
GRAVITY
MAGNETICS
a)
b)
Observed
39
28
17
5
−5
−16
mGals
547
192
−163
−519
−875
−1229
nT
c)
d)
Forward modelled
48
31
14
−1
−18
−35
mGals
814
584
353
123
−107
−337
nT
e)
f)
Inversion misfit
17
10
3
−3
−10
−17
mGals
205
−30
−266
−503
−739
−975
nT
TJI61
19.05.15

Figure 8. (left) a) Bouguer gravity anomaly (mgals) image of the Windimurra Igneous Complex clipped to the area relevant for the inversion volume; b) aeromagnetic (nT) image of the Windimurra Igneous Complex; c) calculated gravity field (mgals) as a result of the forward modelling of 3D Model 3; d) calculated magnetic field (nT) generated as a result of the forward modelling of 3D Model 3; e) gravity field misfit yielded by the inversion; f) magnetic field misfit yielded by the inversion. Note the probable regions of remanence located in the northwest and the south-central parts of the complex. Also note that the east–west trending Proterozoic dyke in the north of the complex is not accounted for in the 3D modelling.

Observations from 10GA-YU2 (CDP 4000–6900)

In map view, seismic line 10GA-YU2 starts in the centre of the western lobe of the complex, proceeds towards the northwestern edge, and, as the line bends around to the east, traverses the middle of the lower zone, and proceeds out to the eastern edge of the complex. At CDP 4422 the line intersects 10GA-YU3 and at CDP 5880 it intersects the end of 10GA-YU1 (Fig. 7b,e).

The dips in the ultramafic zone and lower zone support an interpretation of an overall bowl-shaped vessel for the WIC, with steeper dips at the margins (c. 20°) and subhorizontal reflections in the interior. Since the line approaches the margin of the complex in two places, this bowl shape is duplicated in this section.

The ultramafic zone is imaged along the longest strike length of all the seismic lines and it is considered that the data from this seismic line is representative of the typical thickness of this zone at about 2.1 km. Therefore, in contrast to 10GA-YU3 (next section), it is likely that this line does not image any of the thicker 'root zone' region.

The SDZ is interpreted as a south-dipping horizon towards the southern end of the line, cutting into lower-zone stratigraphy and overlain by middle- and upper-zone material. Very shallow dipping (apparent dip of 0–5°) reflections from CDP 4000 to CDP 4500 are interpreted to represent the magnetitite-rich base of the upper zone, which can be seen to truncate moderately dipping middle zone material (with an apparent dip of 5–15°).

A maximum thickness of 1 km in the line of section is estimated for a shallow, bowl-shaped region above reflective, layered gabbroic rocks at approximately CDP 5800. This is interpreted to be composed of 500 m thickness of the roof zone of the WIC, and 500 m thickness of the overlying Kantie Murdana Volcanics Member.

The Proterozoic Mount Holmes Gabbro sill is interpreted at shallow levels to the east of the complex, and dips 5° to the northeast, as noted in surface outcrops adjacent to the seismic line. This feature is considered to be below the resolution of the 3D model and is therefore not included.

Observations from 10GA-YU3 (CDP 8600–11290)

Seismic line 10GA-YU3 provides an east–west cross-section across the complex from CDP 8800 to CDP 10800 (see Fig. 7c,f). In the west, the line intersects the sheared western contact of the complex along the Challa Shear Zone and continues through to CDP 9308, where it intersects 10GA-YU2. The line then crosses the SDZ, 2 km north of the Windimurra vanadium pit, and continues out past the eastern extent of the complex, across an unexposed contact with metasedimentary rocks within the Wyemandoo Shear Zone. The line finishes in post-tectonic granitic rocks of the Walganna Suite.

The SDZ has an apparent dip which varies from close to horizontal in the central part of the complex to moderately east-dipping in the western part of the complex. At CDP 10000, this zone is cut by a brittle fault, to the east of which the zone dips to the west at approximately 30° apparent dip. Seismic trend lines interpreted within the complex have a shallow dip and form a broadly inward-dipping structure, which is likely related to the primary igneous layering geometry.

The ultramafic zone is interpreted to underlie the lower zone and form a slight keel-shaped region under the centre of the complex down to approximately 3.3s TWT. This is a region of apparently strongly layered ultramafic rocks whose reflectors are partly continuous with other parts of the interpreted ultramafic zone. However, immediately adjacent to this region at shallower depths, there are lower reflectivity units present. These may be due to the presence of a region of strongly serpentinized (and hence more isotropic) ultramafic rocks. Alternatively, the lower reflectivity may be due to structural complexity or granitic intrusions, all of which could account for the discontinuous nature of this region. Our preferred interpretation (Fig. 7f) is that younger granitic rocks intruded at the base of the ultramafic zone; however, it is still considered a region of high uncertainty. In addition, there is potential for this deepest part of the ultramafic zone to be a remnant of a pipe- or funnel-shaped 'root zone' (c.f. 10GA-YU2 where the ultramafic zone appears to have a relatively consistent thickness).

Summary of seismic interpretation

Observations from the three seismic lines provided first order constraints on the thicknesses of various features of the WIC (Table 8).

The following is a list summarizing the features discovered from seismic interpretation:

1. The deepest part of the complex identified is in the central part of its intersection by the 10GA-YU3 seismic line, approximately 10.5 km below the present erosion level. This estimate from seismic data is a minimum estimate (utilizing a velocity of 6000 ms^{-1}) since it is likely that the velocity is >6250 ms^{-1} and hence it may be as deep as 11.5 km. This estimate might not represent the typical thickness of the layered sequence as it may contain a remnant of a pipe-like 'root zone'.

2. The typical thickness of the layered part of the complex away from this potential root zone is estimated at 10.5 km.

3. Seismic data supports the hypothesis that the WIC had an initial shallow conical form. The complex appears relatively intact and coherent in its main part, with local modification by strike-slip shear zones, which have likely steepened layering, at the margins of the complex. In addition, brittle faulting and crosscutting granitic plutons have affected the complex.

4. A two-stage stratigraphy consisting of an eastern and western lobe is permissible given the seismic data; however, it is accepted that it is not clear. Here, we consider the eastern lobe to represent the initial intrusive form, evolving from an ultramafic zone through lower, middle and upper zones. A second lobe (i.e. the western lobe) consistently overlies the eastern lobe when its zones are extrapolated to depth along reflector trend lines. In general, the reflectors are subparallel to the underlying eastern lobe. At the crucial part of 10GA-YU3 (CDP 9500 and 1s TWT) it appears that there is a faulted contact, hence no primary truncation of eastern lobe by western lobe is observed in seismic data even though it is apparent at the surface.

5. Strongly reflective and layered material underlies the entirety of the WIC. This is likely representative of the ultramafic zone, which cannot be traced to the surface using the seismic data. Regions along the northern margin of the complex (e.g. on line 10GA-YU1), however, are identified as having the shallowest parts of this zone at about 600 m depth. The western margin also has a region of shallow (<1 km depth) ultramafic zone material identified at CDP 8800 on 10GA-YU3.

6. The Challa Shear Zone dips approximately 70° to the east-northeast. This dip decreases below 3 km depth to approximately 45°.

7. The interpretation of the SDZ as marking the base of the western lobe of the complex remains plausible as it is consistent with seismic data.

8. An intrusion of a flat slab of ~1 km-thick upper zone material in the western lobe (in the vicinity of the Canegrass Ti–V–Fe prospect) is consistent with seismic data in 10GA-YU2 and 10GA-YU3.

9. A strongly reflective, west-dipping slab (c. 30°) of upper zone material (including the unit at the Windimurra vanadium pit) in the eastern lobe is apparent from seismic data in 10GA-YU3, down to at least 3 km depth.

Table 8. Summary of thickness constraints for the WIC, derived from observations on the Youanmi seismic lines. SDZ = Shephards Discordant Zone, KMVM = Kantie Murdana Volcanics Member. Results are conservative estimates since an average seismic velocity of 6000 ms-1 was used for Archean crust in the published seismic cross-sections. Jones et al. (2012) explain that in the vicinity of the WIC, the velocity is likely closer to 6500 ms^{-1}, yields thicknesses 8.3% higher (i.e. those shown in the final column estimates). Estimates are not made for features that are too thin such as the border zone or the SDZ. Particular estimates are not made for features with minimal information such as the ultramafic and lower zones of the western lobe. Note: zones here are fully subdivided and do not directly match the units in the 3D geomodel.

	Zone	*Max. vertical thickness (km)*	*Max. cumulative perpendicular thickness (km)*	*Maximum depth-to-base (km)*	*Primary source*	*Estimated typical thickness (km) where v = 6.5 kms^{-1}*
Western lobe	KMVM	0.5	0.5	0.7	10GA-YU2	0.5
	Roof	0.3	0.4	0.8	10GA-YU2	0.3
	Western lobe	4.1	5.2	4.1	10GA-YU3	-
	Upper	0.9	1.0	1.4	10GA-YU3	1.0
	Middle	2.3	2.8	3.1	10GA-YU2	2.2
	Lower	1.8	2.0	4.0	10GA-YU3	-
	Ultramafic	-	-	-	-	-
	SDZ	-	-	3.8	10GA-YU3	-
Eastern lobe	Eastern lobe	7.9	9.7	10.5	various	9.5
	Upper	0.7	0.8	2.6	10GA-YU3	0.6
	Middle	0.9	1.0	3.0	10GA-YU3	0.9
	Lower	6.1	6.3	6.2	10GA-YU2	5.7
	Ultramafic	3.2	3.2	10.5	10GA-YU3	2.3
	Border zone	-	-	-	-	-
	WIC as a whole	10.1	13.7	10.5	10GA-YU3	11.4

10. The Kantie Murdana Volcanics Member is just distinguishable from underlying units and appears to overlie up to 1 km thickness of gabbroic rocks of the roof zone of the complex (as visible in high-resolution seismic data on 10GA-YU2 presented in Wyche et al., 2014). Hence, both of these units overlie and truncate the seismically layered rocks of the eastern lobe of the complex.

Results from 3D modelling

Initial results and refinement

Model 1 — simple geology model

An initial model was created which prioritized structural data from the well-preserved (i.e. away from shear zones) parts of the WIC with primary igneous layering. Large-scale geometric relations in seismic data from the various zones of the complex were also incorporated, and it was possible to create a model which extrapolates these data in 3D without the introduction of structural complexity. Hence, results of a simplified geological 3D model prior to the introduction of faults yielded Model 1, which fitted selected and well-constrained map and seismic data in the core of the complex only. In the periphery of the complex there were discrepancies relative to surface mapping constraints and volume estimates from the subsequent 3D models as follows: (1) The western lobe of the complex (i.e. that which lies above the SDZ) extends ~30 km further west of the Challa Shear Zone and occupies approximately three times the volume indicated from successive models (Table 9); (2) The lower zone extends west and occupies approximately 2.5 times the volume of successive models. Similarly, the ultramafic zone is approximately 1.6 times the volume and extends further west; (3) The ultramafic zone projects to the surface with an outcrop approximately 4 km wide concentrically around the eastern lobe of the complex; (4) The total volume modelled for the WIC without faults is approximately double that of successive models, indicating that the initial volume of the complex may have been in the vicinity of 26 000 km^3. Admittedly, this volume estimate is quite poorly constrained; however, we consider it the best estimate possible with the present 3D data. It also represents an estimate of the original shape of the intrusion.

Table 9. The volumes of the various modelled units in Models 1 and 2. Note: only Model 3 is shown in the 3D geomodel

Unit	*Model 1 volumes (km^3)*	*Model 2 volume (km^3)*
S02_KantieMV_RoofZone		63
S03_UpperMiddleZonesWest		357
S04_ShephardsDiscordantZone'	4 050	2 360
S05_UpperMiddleZonesEast	11 400	740
S06_LowerZoneEast'		6 252
S07_Ultramafic	10 800	3 803
TOTAL	26 250	13 155

Model 2 — addition of shear zones

The discrepancies listed above were readily resolved in Model 2, first by the introduction of the Challa Shear Zone at the western margin of outcrop of the complex. This fault was allowed to displace the complex entirely above surface to the west of the fault. The result of this was that a large area of high gravity to the west of the fault (the Muleryon Hill area) was occupied by granitic rocks in the model, therefore changes were made so that the ultramafic zone was not entirely displaced and hence allowed to outcrop under the Challa salt lake area (including the known exposures of ultramafic rocks of Muleryon Hill). Second, shear zones along the east (unnamed shear zone) and northwest (Yarloo Shear Zone) of the complex were introduced using surface constraints on their orientation in order to remove outcropping ultramafic zone rocks along these marginal areas. Third, a 'post-tectonic granite' (Bald Rock Supersuite) was introduced at the southern margin in order to truncate the zones of the complex as shown in Fig. 2. The resultant 3D map produced was Model 2 which accounted for the internal and external form of the complex given surface and seismic constraints (resultant volumes shown in Table 9). Forward modelling (see later) suggested modifications were required to account for the geometry of the central part of the complex

Forward modelling and the final 3D model

Model 3 — forward modelled

A smaller volume within the GeoModeller project was used for forward modelling and inversion (Figs 3 and 8a,b; Table 10). This enabled focus on the WIC and avoidance of high-density and high-magnetic regions in the vicinity of Mount Magnet and Youanmi townsites that were not modelled in 3D. It also reduced the time taken for each forward model/inversion run. The approach adopted here was to use available geometric and physical property constraints (as previously described) to produce an initial forward model. Minor adjustments to the physical properties were required for poorly constrained or unknown units such as the ultramafic zone and basement granites in order to yield a first order fit for magnetic and gravity survey data. Following this, better fits were achieved by modifying the model geometry.

Table 10. Maximum and minimum values in the coordinate system MGA zone 50 for the modelled volume in metres

	Minimum	*Maximum*
X	605 000	665 000
Y	6 822 000	6 934 000
Z	-20 000	450

This was changed in simple ways and in selected regions with higher degrees of freedom (i.e. away from known geometric constraints from surface or seismic observations). The result of this iterative process was to achieve a reasonable forward-modelled fit to potential field data given the resolution and other limitations of the 3D model.

The forward model result of Model 2 at 2 x 2 x 1 km resolution produced a sharp high-density area in the central region of the complex whereby the upper zones for both lobes of the complex overlay each other. The geometry of the eastern lobe was therefore simplified at depth so that middle and upper zones were more gradually curved. This resulted in a geometry whereby these zones did not underlie the Kantie Murdana Volcanics Member to any significant extent. The western lobe also attained a simpler geometry with a slight reduction in its volume. The modifications were in a region that was relatively unconstrained by seismic data, which also had poor exposure; therefore, it was deemed a feasible adjustment to make.

Model 3 resulted from the adjustments described above and minor modifications in the thickness of various units in order to produce a good fit to potential field data. The results are shown in Figure 8c and d, Table 11, indicating that the large reduction in middle and upper zones of the eastern lobe (i.e. 'MiddleZone') was accommodated primarily by increased lower zone material. This fit (i.e. relatively low degree of mismatch) was deemed sufficient given the inherent limitations of the 3D model in general, especially in terms of resolution (as discussed earlier).

Table 11 shows the final volumes for Model 3 and that the lower zone of the eastern lobe accounts for approximately half the volume of the entire complex. A conservative estimate for the volume of the WIC as a whole is therefore c. 13 000 km^3.

Inversion

In order to refine and test the implications of Model 3, a geophysical inversion was run to provide a statistical appraisal of the success or failure of aspects of the implied geometry. 3D GeoModeller uses a stochastic inversion process to alter either the modelled lithological boundaries or properties within specified constraints with a set 15% chance of a property or geometry change. This process requires a starting model (Model 3) which can closely reproduce the observed geophysical responses. Joint inversions were run on Model 3 utilizing detrended gravity and aeromagnetic grids using the parameters outlined in Table 12. Voxel sizes of between 2 and 0.5 km were used as the resolution of the model was 1 km; however, it was found that more accurate results in the region of the relatively thin Kantie Murdana Volcanics Member required a smaller voxel size of 0.5 km.

Table 13 shows that some significant lithological voxel changes (i.e. substitution of lithologies of different densities) were required by the final inversion run. This is the result of one major change, that basement granitic rocks of low density were required to replace a significant proportion of the ultramafic zone of the complex. This is relatively straightforward to reconcile with seismic observations in that granitic sills parallel to layering of the ultramafic zone would be consistent with the strongly layered seismic character of this zone. There was also a shift to reduce the proportion of other high-density lithologies of the middle and upper zones of both the eastern and western lobes, which may be due to overestimates of their densities.

Table 11. The volumes of the various modelled units in Model 3

Unit	*Model 3 volume (km^3)*	*Model 3 – Model 2 (%)*
V01_BaldRockSupersuite	1 258	
V02_KantieMV_RoofZone	108	
V03_UpperMiddleZonesWest	386	+7%
V04_LowerZoneWest	2 170	-9%
V05_UpperMiddleZonesEast	589	-26%
V06_LowerZoneEast	6 415	+3%
V07_UltramaficZone	4 162	+9%
V08_Metagranites_Basement	39 509	
V09_YarraquinSeismicProvince	82 827	

Table 12. Inversion parameters for runs 1–4

Inversion run	*Voxels #*	*Voxel size (km)*	*P(lith change) %*	*P(voxel in model)%*
1	30 x 56 x 20	2 x 2 x 1	50	Uncon-strained
2	30 x 56 x 20	2 x 2 x 1	0	100
3	60 x 112 x 41	1 x 1 x 0.5	25	84
4	60 x 112 x 41	1 x 1 x 0.5	50	70

Table 13. The volumes of the various modelled units in Model 3 compared to inversion results

Unit	*Model 3 inversion volume (km^3)*	*Model 3 inverted – Model 3 initial (km^3)*	*Model 3 inverted – Model 3 initial (vol. % change)*
V01_BaldRockSupersuite	1 027	-131	-10%
V02_KantieMV_RoofZone	92	-16	-15%
V03_UpperMiddleZonesWest	335	-50	-13%
V04_LowerZoneWest	2 310	+143	+6%
V05_UpperMiddleZonesEast	178	-411	-70%
V06_LowerZoneEast	6 700	-285	-4%
V07_UltramaficZone	1 624	-2538	-60%
V08_Metagranites_Basement	44 773	5264	+13%
V09_YarraquinSeismicProvince	80 382	-2445	-3%

Discussion

Implications of the first order data and constraints

Thickness estimates

The stratigraphic thickness estimated for the combined eastern and western lobes of the WIC is approximately 11 km, which is thicker than that estimated for the 8 km-thick Rustenberg Layered Series of the Bushveld Igneous Complex (Cawthorn and Walraven, 1998), previously the thickest such sequence of layered gabbroic rocks identified. This 11 km estimate may be too high for several reasons. (1) If the eastern and western lobes are considered separate but overlapping intrusions, then 11 km represents a combined thickness. However, the eastern lobe would still show a vertical thickness of between 9 and 10 km, which is still extremely thick. The revised stratigraphic column is presented in Figure 9 and is the result, primarily of seismic data (Ivanic et al., 2014); (2) Structural repetition may cause some enhanced thickening of the central parts of the complex. Very small-scale reverse faults have been noted in the Windimurra vanadium pit in the eastern lobe of the complex; however, these are not thought to be responsible for large-scale duplication and the thickening associated with them is thought to be minor; (3) A downwarping of the entire complex could artificially enhance the thickness in the centre of the complex. Some evidence of this has been noted — for example, a synformal axial trace in the northern part of the eastern lobe (Ivanic, 2012b) but this is unlikely to contribute more than a few hundred metres of enhanced thickness; (4) It is possible that some of the highly reflective material at the base of the ultramafic zone in 10GA-YU3 is part of a feeder funnel at the base of the complex. Inclusion of this in the total thickness is deemed reasonable as there are contiguous layered rocks within and above this region; (5) Minor addition of gabbroic material into the layered sequence by sills assigned to the Warakurna Supersuite may have contributed up to 100 m in thickness locally. Therefore, even allowing for these points, the thickness of the complex as a whole is still likely to be in the region of 11 km. Furthermore, several factors may be reducing this estimate of the thickness such as normal faulting, erosion from the top and intrusion of granites from beneath.

This vast thickness suggests that there may have been something fundamentally different about the WIC, compared to proximal Archean intrusions and subsequent examples of Proterozoic–Phanerozoic intrusions. We speculate that it was the superimposed, multipulsed nature of the developing cumulate sequence that allowed for a dominance of vertical accumulation over lateral spread.

Thermomechanical modelling of the dynamics of magma emplacement suggest a transition from vertical to horizontal flow for large intrusions at the brittle–ductile transition (Brown, 2007 and references therein). Therefore, the depth of the base of the complex potentially provides an estimate for the brittle ductile transition at 2810 Ma of about 11 km. This estimate is probably reasonable, since the elevation of the upper contact is also constrained by the presence of the Kantie Murdana Volcanics Member above the central parts of the complex.

Discordance

The subdivision of the WIC into an eastern and western lobe along the SDZ is consistent with surface observations of magmatic discordance between the two lobes (Ahmat, 1986). The lack of deformation features in this zone, in addition, strongly argues for a nondeformational origin. The interpretation presented here of the SDZ extending across to the west at depth and entirely subdividing the complex is also consistent with seismic interpretations and 3D constraints. The implication of this is that, rather than being an isolated region of discordance of a structural or magmatic nature (Ahmat, 1986), it is implicitly a large and significant subdivision of the complex, reflecting the later timing (within the error of geochronological data) and crosscutting nature of the western lobe.

In this interpretation, the SDZ is positioned whereby it represents the uppermost part of the eastern lobe in 3D. Along its eastern contact, there is little or no discordance with igneous stratigraphy of the eastern lobe, whereas on the western margins of the SDZ, as one follows from the southern extent of the complex to the north, a traverse is made up the igneous stratigraphy of the western lobe from the central part of the lower zone to the upper part of the middle zone (Fig. 2; i.e. several kilometres of discordance compared to the eastern lobe). Then to the northwest, the SDZ is itself truncated by the roof zone and Kantie Murdana Volcanics Member. Finally, to the west, it re-emerges at the surface and represents the lowermost upper zone of the western lobe, where it directly overlies the lower zone of the eastern lobe. This geometry runs into the crosscutting Challa Shear Zone at the western margin of the WIC. At depth, these constraints are maintained underneath the entire western lobe where it is underlain by variable thicknesses of ultramafic and lower zone sequences of the eastern lobe.

Small-scale discordance as observed in 10 m to 1 km features in the field (Ahmat, 1986; Ivanic et al., 2014) were not considered in this interpretation and on a macro-scale, the eastern lobe is not considered to show the type of discordances found in the western lobe. Progressing up-stratigraphy into the western lobe, its middle zone as a whole shows a transgressive discordant geometry, whereby at the surface it cuts across and entirely truncates the lower zone of the western lobe to the east (complete truncation occurs about 5 km south of the Windimurra vanadium pit).

The crosscutting nature of the upper zone of the western lobe (Nebel et al., 2013b) is exemplified in the seismic and 3D interpretation presented here (Figs 7, 9 and 10; Appendix 3D model). This zone is interpreted to cut down into all underlying igneous stratigraphic units, for example into the lower zone of the eastern lobe (on 10GA-YU2 at CDP 4570; Fig. 7e). At the surface, the middle zone of the western lobe is entirely overstepped by the upper zone (Fig. 2) both at its northern and southern limits.

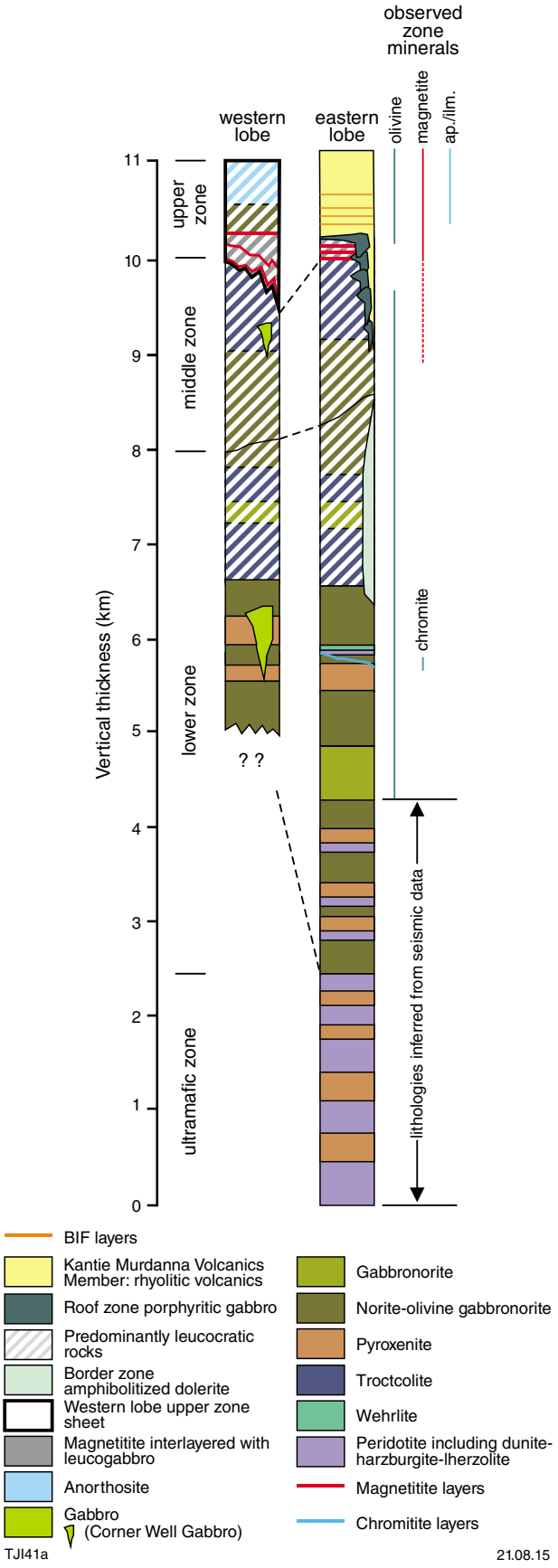

Ultramafic zone

The two-fold subdivision of the complex brings into question the presence of an ultramafic zone for the western lobe, which has not previously been defined. In the 3D model the ultramafic zone is not separated into eastern and western portions and is interpreted to underlie the entire complex. One possibility is that the ultramafic zone of the western lobe is distinct from that of the eastern lobe and underlies the southwestern part of the complex, where it is not exposed and has not been imaged by the southerly extensions of the seismic lines. In general, the details of the form of the western lobe still remain relatively unconstrained in 3D owing first to the lobe's significant truncation by the Challa Shear Zone to the west; hence, this lobe's ultramafic zone may have been removed. Second, there is a lack of seismic data further south and third, there is a lack of rock exposure especially around the Challa Salt Lake system.

A significant ultramafic zone is likely to underlie the entire complex with a thickness of 1–2 km and possibly as much as 3 km. The presence of this basal component of the WIC effectively accounts for the 'missing ultramafic zone' (Ahmat, 1986; Ivanic et al., 2010), and therefore mitigates against the possibility (Bunting, 2004) that the Narndee Igneous Complex represents the ultramafic portion of the WIC. The bulk composition of the WIC is, therefore, much less Ca- and Al- rich than previously anticipated (Ahmat, 1986) and closer to a tholeiitic/komatiitic basalt composition.

There also remains the possibility that remnants of the original feeder system exist underneath the central part of the complex as highlighted in the 10GA-YU3 seismic line in 2D. This region is likely intruded by granitic rocks, rendering its precise form untraceable in 3D. Reflectors in 10GA-YU3 do, however, hint at a funnel-shaped form which may well become more significant out of the plane of this line towards the south.

Figure 9. **(left) Revised igneous stratigraphic column for the Windimurra Igneous Complex (see Fig. 6), showing true thickness for all major components of the complex as derived from observations made at the surface and from 3D modelling. The Complex is divided into an eastern and western lobe along the Shephards Discordant Zone (dashed correlation lines, indicating an offset in stratigraphy). The ultramafic zone is interpreted from seismic data alone. Note also the major oxide horizons of chromite-rich and magnetite-rich rock types.**

Implications of the inversion results

The results of the geophysical inversion yielded some implications, which are primarily that the large-scale geometry, in the upper parts of the complex at least, is consistent with geophysical data. However, specific excursions from the initial geometry of the 3D model were implied by the geophysical inversion (Table 13), which resulted in the replacement of high-density lithologies with lower density ones. There may be several reasons for this tendency. First, the densities of the ultramafic and magnetite-rich rocks may have been overestimated. For example, as the ultramafic zone has not been directly sampled, it may contain a significant proportion of pyroxenite or gabbroic rocks, reducing its average density. Likewise, the upper zone of the western lobe may have been assigned higher density and magnetic susceptibility values owing to utility of diamond drillhole data, which primarily samples the magnetite-rich lower part of the upper zone.

Second, there may be a significant intrusion of granitic rocks into the ultramafic zone as indicated by the inversion voxels in this region. These granitic rocks may belong to the Big Bell or Tuckanarra Suites, or alternatively they may be an extension of the Walganna Suite rocks inferred to intrude at the base of the complex in 10GA-YU3 (Fig. 7f). In addition, significant serpentinization may also account for a density reduction of the ultramafic zone especially in proximity to major shear zones.

Third, there may be a geometric inaccuracy in the model; however, this is unlikely in the upper zone as it is well constrained by surface and seismic observations. Lacking further constraints, the form of the ultramafic zone may be more irregular than that estimated from seismic data alone and it could possess a more restricted funnel region compared with the 3D model.

Our assessment of these implications is that we have likely overestimated the density of the upper zones of the eastern and western lobes. In addition, we infer that the density of the ultramafic zone may also have been overestimated; however, it is likely that our estimation of the volume of granitic intrusions into this zone was underestimated.

Evidence for a genetic model

From the geometric constraints described above, the overall emplacement sequence is envisaged as follows (Fig. 10a; Stages 1–2): Stage 1: incipient emplacement including formation of chilled margins represented by the border zone dolerites and potentially a 'root zone' as a funnel-shaped feeder system at depths in excess of 10 km below the present-day erosion level; Stage 2: emplacement of the layered sequence of ultramafic, lower, middle and upper zones of the bowl-shaped eastern lobe, a multipulsed fractional crystallization sequence; (Fig. 10b; Stages 3–5) Stage 3: west-down tilting of the eastern lobe, possibly ~10°; Stage 4: emplacement of the magma of the western lobe. Initially an ultramafic postulated to have developed at depth with the lower zone up against magnetitites of the upper zone of the eastern lobe along the SDZ. These magnetitites (likely still hot as no clear chilled margin exists) may have acted as an impenetrable barrier to this incursion; however, these appear cut across in the north of the complex; Stage 5: fractional crystallization and continued pulsed inflation of the western lobe leading to emplacement of its middle zone with an erosive base; (Fig. 10c; Stages 6 and 8) Stage 6: emplacement of the upper zone of the western lobe as a single pulse of extremely Fe-enriched magma with extreme discordance to all underlying units. Northwest–southeast trending density currents likely created the channel features of thicker magnetitites present in the Canegrass region. These apparently scoured deeper into the middle zone in this vicinity probably owing to their more central position as a result of down-dip density currents sourced from the southeast; Stage 7 (not shown on figure): intrusion of the Corner Well Gabbro pipes probably sourced from a final phase of low-volume primitive melt underlying the complex; Stage 8: extrusion of the overlying Kantie Murdana Volcanics Member and emplacement of the roof zone gabbroic plutons, which intrude and chill at the base of the volcanics; (Fig 10d; Stage 9) Stage 9: post 2813 Ma events. These are dominantly granitic intrusions; deformation along the Challa Shear Zone and Wyemandoo Shear Zone; brittle internal deformation of the WIC; Proterozoic dykes and sills (not shown on figure); erosion to present-day level.

With this genetic model as a base, future work may be able to test the validity of several of these proposed stages for the evolution of the WIC. Given that this is, in the most part, a deformed and metamorphosed intrusion, future work will require more detailed geophysical analysis and further isotopic work in order to document the nuances of the finer scaled layering geometry and timing of emplacement for the various units.

Conclusions

A preliminary 3D model for the complex was generated using GeoModeller, and incorporated map data and geophysical survey data as well as preliminary interpretation of the three seismic lines (see data: 3D geomodel). The model yielded a 3D form for the zones of the intrusion that is consistent with surface and seismic data. The model confirmed the broad funnel-shaped form and the inward-dipping nature of the main subdivisions of the complex.

1. The WIC is the world's thickest mafic–ultramafic layered intrusion reported at 10.5 km. This estimate from seismic data is a minimum estimate (utilizing a velocity of 6000 ms^{-1}) since it is likely that the velocity is >6250 ms^{-1} and hence it may be as thick as 11.5 km.

2. A two-fold stratigraphy for the complex with an eastern and western lobe is required to accommodate 3D constraints presented here. The eastern lobe represents the initial intrusive form evolving from an ultramafic zone through the lower, middle and upper zone. Subsequently, the western lobe intruded in the south west, and cut across the lower, middle and upper zones of the eastern lobe.

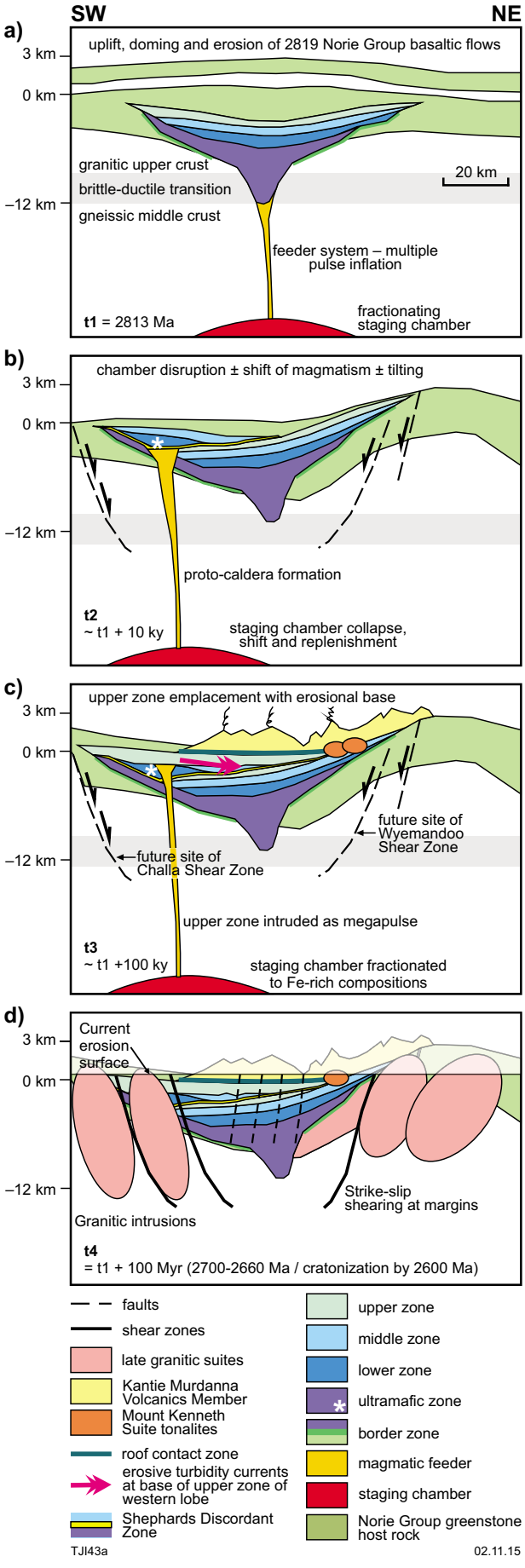

3. 3D inversions show that a significant ultramafic zone, approximately 3 km thick at its maximum, likely underlies the entire complex. The bulk composition is, therefore, much less Ca- and Al- rich than previously anticipated and closer to a tholeiitic/komatiitic basalt composition. Contiguous parts of the ultramafic zone of the complex are modelled to be within 500 m of the surface along its northwestern margins.

4. Possibly as much as half of the original western lobe of the complex was faulted off to the west by the Challa Shear Zone according to our Model 1. The original volume of the complex as a whole is estimated at about 26 000 km^3. The location of this missing volume is unknown, but likely eroded.

5. The ultramafic zone likely extended to the surface around most of the complex prior to deformation. It is also likely to occur as a lens along a north northwest-trending, 20 km strike length of the Challa Shear Zone, resulting in the extended gravity high west of the main outcrop of the complex. Therefore, the rocks of the Muleryon Hill area are thought to belong to the WIC rather than the Narndee Igneous Complex.

6. Identification of the thick, subsurface ultramafic zone underlying the lower zone of the eastern lobe of the complex is a new target for Ni–Cr–PGE mineralization.

7. Extension of the SDZ to the west of the complex provides a 3D geometry consistent with geophysical data. This zone is cut by the upper zone of the western lobe in the north. It is also truncated in the north by the roof zone and the overlying Kantie Murdana Volcanics Member.

8. A modelled shallow-dipping, low-curvature slab of 1 km thick upper zone material from the western lobe in the vicinity of the Canegrass Ti–V–Fe prospect is consistent with geophysical data.

9. In the vicinity of the Windimurra vanadium pit, a modelled moderately west-dipping slab of upper zone material from the eastern lobe is consistent with geophysical data.

10. The Kantie Murdana Volcanics Member is modelled at 0.5 km thick, overlying up to 1 km thickness of relatively dense gabbroic rocks of the roof zone of the complex.

Figure 10. (left) Schematic genetic model for the formation of the Windimurra Igneous Complex (see text for discussion). a) Initial stage of intrusion into the Norie Group (t1), formation of the eastern lobe; b) formation of the western lobe (t2); c) formation of the upper zone of the eastern lobe, Mount Kenneth Suite and Kantie Murdana Volcanics Member (t3); d) formation of granitic rocks of the Big Bell Suite, Tuckanarra Suite and Bald Rock Supersuite and deformation and erosional features (t4). White asterisks in b) and c) denote possible site of ultramafic zone of western lobe now removed by shearing.

Acknowledgements

The Youanmi seismic interpretation workshops held in 2013 involved diverse discussions concerning many facets of the geophysics and geology in the vicinity of the WIC. Leonie Jones provided seismic processing refinements in the vicinity of the WIC. The following are thanked in particular for contributions that helped shape our views presented here: Richard Blewett, Stephen Wyche, Russell Korsch and Brian Kennett. In addition, John Bunting and Graham Kennedy are thanked for useful discussions on the formation of the Windimurra Igneous Complex. Craig O'Neil (Macquarie University) is acknowledged for analysis of rock properties shown in Table 3.

This manuscript has benefited from helpful discussions with Klaus Gessner and David Howard, and thorough reviews from Heather Howard and Ruth Murdie at the Geological Survey of Western Australia.

References

Ahmat, AL 1986, Petrology, structure, regional geology and age of the gabbroic Windimurra complex, Western Australia: The University of Western Australia, Perth, PhD thesis (unpublished), 279p.

Ahmat, AL and De Laeter, JR 1982, Rb–Sr isotopic evidence for Archaean–Proterozoic crustal evolution of part of the central Yilgarn Block, Western Australia: constraints on the age and source of the anorthositic Windimurra Gabbroid: Journal of the Geological Society of Australia, v. 29, p. 177–190.

Brown, M 2007, Crustal melting and melt extraction, ascent and emplacement in orogens: mechanisms and consequences: Journal of the Geological Society, v. 164, p. 1–22.

Bunting, JA 2004, The nickel–PGE potential of the Narndee and Windimurra intrusions; Apex Minerals NL: Geological Survey of Western Australia, Statutory mineral exploration report, A69643 (unpublished).

Cawthorn, RG and Walraven, F 1998, Emplacement and crystallization time for the Bushveld complex: Journal of Petrology, v. 39, no. 9, p. 1669–1687, doi:10.1093/petroj/39.9.1669.

Costelloe, RD and Jones, LEA 2014, Youanmi seismic survey 2010: acquisition and processing, *in* Youanmi and southern Carnarvon seismic and magnetotelluric (MT) workshop 2013 *compiled by* S Wyche, TJ Ivanic and I Zibra: Geological Survey of Western Australia, Perth, Record 2013/6, p. 1–6.

Gill, M 2011, The petrogenesis and FeTiO accumulation of the Youanmi Igneous Complex (Yilgarn Craton), Western Australia: University of Tasmania, Honours thesis (unpublished).

Ivanic, TJ 2009, Madoonga, WA Sheet 2444: Geological Survey of Western Australia, 1:100 000 Geological Series.

Ivanic, TJ 2011, Coolamaninu, WA Sheet 2540: Geological Survey of Western Australia, 1:100 000 Geological Series.

Ivanic, TJ 2012a, Challa, WA Sheet 2541: Geological Survey of Western Australia, 1:100 000 Geological Series.

Ivanic, TJ 2012b, Windimurra, WA Sheet 2641: Geological Survey of Western Australia, 1:100 000 Geological Series.

Ivanic, TJ 2014, Youanmi, WA Sheet 2640: Geological Survey of Western Australia, 1:100 000 Geological Series.

Ivanic, TJ, Korsch, RJ, Wyche, S, Jones, LEA, Zibra, I, Blewett, RS, Jones, T, Milligan, P, Costelloe, RD, Van Kranendonk, MJ, Doublier, MP, Hall, CE, Romano, SS, Pawley, MJ, Gessner, K, Patison, N, Kennet, BLN and Chen, SF 2014, Preliminary interpretation of the 2010 Youanmi deep seismic reflection lines and magnetotelluric data for the Windimurra Igneous Complex, *in* Youanmi and southern Carnarvon seismic and magnetotelluric (MT) workshop 2013 *compiled by* S Wyche, TJ Ivanic and I Zibra: Geological Survey of Western Australia, Perth, Record 2013/6, p. 97–111.

Ivanic, TJ, Wingate, MTD, Kirkland, CL, Van Kranendonk, MJ and Wyche, S 2010, Age and significance of voluminous mafic–ultramafic magmatic events in the Murchison Domain, Yilgarn Craton: Australian Journal of Earth Sciences, v. 57, p. 597–614.

Jones, LEA, Ivanic, TJ and Costelloe, RD 2012, Seismic reflection imaging of the mafic–ultramafic Windimurra Igneous Complex, Yilgarn Craton, Western Australia, *in* Extended abstracts volume: 22nd Australian Society of Exploration Geophysicists international conference and exhibition, Brisbane, Australia, 26 February 2012, p. 1–4.

Korsch, RJ, Blewett, RS, Wyche, S, Zibra, I, Ivanic, TJ, Doublier, MJ, Romano, SS, Pawley, MJ, Johnson, SP, Van Kranendonk, MJ, Jones, LEA, Kositcin, N, Gessner, K, Hall, CE, Chen, SF, Patison, N, Kennett, BLN, Jones, T, Goodwin, JA, Milligan, P and Costelloe, RD 2014, Geodynamic implications of the Youanmi and southern Carnarvon deep seismic relection surveys: a ~1300 km traverse from the Pinjarra Orogen to the eastern Yilgarn craton, *in* Youanmi and southern Carnarvon seismic and magnetotelluric (MT) workshop 2013 *compiled by* S Wyche, TJ Ivanic and I Zibra: Geological Survey of Western Australia, Perth, Record 2013/6, p. 147–166.

Nebel, O, Arculus, RJ, Ivanic, TJ and Nebel-Jacobsen, YJ 2013a, Lu–Hf isotopic memory of plume–lithosphere interaction in the source of layered mafic intrusions, Windimurra Igneous Complex, Yilgarn Craton, Australia: Earth and Planetary Science Letters, v. 380, p. 151–161.

Nebel, O, Arculus, RJ, Ivanic, TJ, Rapp, R and Wills, KJA 2013b, Upper Zone of the Archean Windimurra layered mafic intrusion, Western Australia: insights into fractional crystallisation in a large magma chamber: Journal of Mineralogy and Geochemistry, v. 191, no. 1, p. 83–107.

Nebel, O, Mavrogenes, JA, Arculus, RJ, Ivanic, TJ and Langford, R 2010, Geochemical depth-profiling of late-stage melts from the ~2.8 Ga Windimurra Igneous Complex, Western Australia, in Abstracts: Fifth International Archean Symposium, Perth, 5 September 2010, 4p.

Nelson, DR 2001, 169003: vesicular rhyolite, Carron Hill; Geochronology Record 170: Geological Survey of Western Australia, 4p.

Parks, J 1998, Weld Range platinum group element deposit, *in* Geology of Australian and Papua New Guinean mineral deposits *edited by* DA Berkman and DH Mackenzie: The Australian Institute of Mining and Metallurgy, Monograph 22, p. 279–286.

Scowen, PAH 1991, The geology and geochemistry of the Narndee intrusion: Australian National University, Canberra, Australian Capital Territory, PhD thesis (unpublished), 214p.

Van Kranendonk, MJ, Ivanic, TJ, Wingate, MTD, Kirkland, CL and Wyche, S 2013, Long-lived, autochthonous development of the Archean Murchison Domain, and implications for Yilgarn Craton tectonics: Precambrian Research, v. 229, p. 49–92.

Wang, Q 1998, Geochronology of the granite–greenstone terranes in the Murchison and Southern Cross Provinces of the Yilgarn Craton, Western Australia: Australian National University, Canberra, PhD thesis (unpublished), 186p.

Wingate, MTD, Kirkland, CL and Ivanic, TJ 2012, 194747: metagabbro, Malamiter Well; Geochronology Record 1013: Geological Survey of Western Australia, 4p.

Wyche, S, Ivanic, TJ and Zibra, I (compilers) 2014, Youanmi and southern Carnarvon seismic and magnetotelluric (MT) workshop: Geological Survey of Western Australia, Record 2013/6, 180p.

Wyche, S, Kirkland, CL, Riganti, A, Pawley, MJ, Belousova, E and Wingate, MTD 2012, Isotopic constraints on stratigraphy in the central and eastern Yilgarn Craton, Western Australia: Australian Journal of Earth Sciences, v. 59, no. 5 (Archean evolution — Yilgarn Craton), p. 657–670, doi:10.1080/08120099.2012.697677.

Wyman, DA and Kerrich, R 2012, Geochemical and isotopic characteristics of Youanmi terrane volcanism: the role of mantle plumes and subduction tectonics in the western Yilgarn Craton: Australian Journal of Earth Sciences, v. 59, no. 5 (Archean evolution — Yilgarn Craton), p. 671–694, doi:10.1080/08120099.2012.702684.

Zibra, I, Ivanic, TJ and Chen, SF 2013, Wynyangoo, WA Sheet 2542: Geological Survey of Western Australia, 1:100 000 Geological Series.

RECORD 2015/12

THE WINDIMURRA IGNEOUS COMPLEX, YILGARN CRATON: AN ARCHEAN LAYERED INTRUSION REVEALED BY SEISMIC DATA AND 3D MODELLING

Ivanic and Brett

This Record is published in digital format (PDF) and is available as a free download from the DMP website at <www.dmp.wa.gov.au/GSWApublications>.

Further details of geological products produced by the Geological Survey of Western Australia can be obtained by contacting:

Information Centre
Department of Mines and Petroleum
100 Plain Street
EAST PERTH WESTERN AUSTRALIA 6004
Phone: +61 8 9222 3459 Fax: +61 8 9222 3444
www.dmp.wa.gov.au/GSWApublications